
TiRex: Zero-Shot Forecasting Across Long and Short Horizons with Enhanced In-Context Learning

Andreas Auer^{1,2}
Sebastian Böck¹

Patrick Podest²
Günter Klambauer^{1,2}

Daniel Klotz³
Sepp Hochreiter^{1,2}

¹NXAI GmbH, Linz, Austria

²ELLIS Unit, LIT AI Lab, Institute for Machine Learning, JKU Linz, Austria

³Interdisciplinary Transformation University Austria, Linz, Austria

Abstract

In-context learning, the ability of large language models to perform tasks using only examples provided in the prompt, has recently been adapted for time series forecasting. This paradigm enables zero-shot prediction, where past values serve as context for forecasting future values, making powerful forecasting tools accessible to non-experts and increasing the performance when training data are scarce. Most existing zero-shot forecasting approaches rely on transformer architectures, which, despite their success in language, often fall short of expectations in time series forecasting, where recurrent models like LSTMs frequently have the edge. Conversely, while LSTMs are well-suited for time series modeling due to their state-tracking capabilities, they lack strong in-context learning abilities. We introduce TiRex that closes this gap by leveraging xLSTM, an enhanced LSTM with competitive in-context learning skills. Unlike transformers, state-space models, or parallelizable RNNs such as RWKV, TiRex retains state-tracking, a critical property for long-horizon forecasting. To further facilitate its state-tracking ability, we propose a training-time masking strategy called CPM. TiRex sets a new state of the art in zero-shot time series forecasting on the HuggingFace benchmarks *GiftEval* and *Chronos-ZS*, outperforming significantly larger models including *TabPFN-TS* (Prior Labs), *Chronos Bolt* (Amazon), *TimesFM* (Google), and *Moirai* (Salesforce) across both short- and long-term forecasts.

1 Introduction

Recent research in time series forecasting has adopted in-context learning through large-scale pre-trained models, analogous to large language models (Woo et al., 2024; Ansari et al., 2024a; Das et al., 2024). These models enable zero-shot forecasting, allowing them to generalize to unseen datasets without parameter updates, akin to meta-learning Hochreiter et al. (2001). This capability empowers practitioners without machine learning expertise to use advanced forecasting tools. More importantly, zero-shot forecasting significantly improves performance in data-scarce settings, where training task-specific models often fail to generalize. As a result, in-context learning models hold promise for broad adoption in domains such as energy, retail, or healthcare.

Most pre-trained time series models are based on transformer architectures (Vaswani et al., 2017), which are well suited for in-context learning, but despite their success in language, often fall short of expectations in time series forecasting (e.g., Zeng et al., 2023). In contrast, LSTMs (Hochreiter, 1991; Hochreiter & Schmidhuber, 1997) have demonstrated strong results in time series forecasting due to their recurrence and effective state-tracking (e.g., Nearing et al., 2024). Therefore, LSTMs are more expressive than state-space models (SSMs), parallelizable RNNs like RWKV (Peng et al., 2023), and transformers (Merrill & Sabharwal, 2023; Merrill et al., 2024; Delétang et al., 2023). However, they

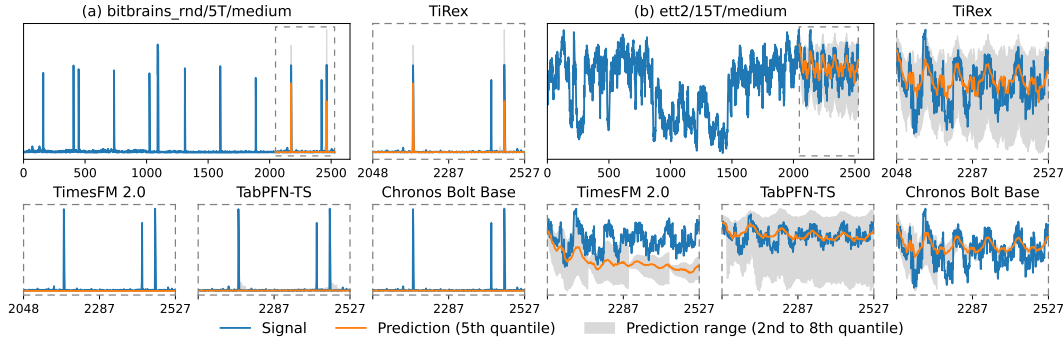


Figure 1: Two exemplary time series from the GiftEval benchmark. For both examples, we show one plot with the full context and TiRex’s prediction, as well as zoomed-in forecasts of the best-performing zero-shot models. Each plot shows the signal in blue, the model’s (median) prediction in orange, and the uncertainty bounds in gray. (a) A time series that exhibits strong peaks. Only TiRex is capable of predicting the periodic short spikes. (b) A time series with strong but noisy periodical behavior. TiRex predicts a meaningful uncertainty estimate (quantile range) over the long forecast horizon, while TimesFM and Chronos Bolt struggle because of collapsing quantiles.

lack strong in-context learning capabilities. To bridge this gap, we adopt xLSTM (Beck et al., 2024), a modern LSTM variant that incorporates architectural enhancements for scalability and improved generalization. In particular, xLSTM has demonstrated in-context learning performance comparable to that of transformer-based large language models (Beck et al., 2025).

To fully unlock xLSTM’s state-tracking abilities, we introduce Contiguous Patch Masking (CPM), a novel training-time masking strategy. CPM enhances xLSTM’s ability to produce coherent long-horizon predictions by mitigating degradation common in autoregressive multi-step forecasting, as illustrated in Figure 1.

While synthetic datasets are frequently used for pre-training forecasting models, the potential of data augmentation strategies remains largely untapped, unlike their established role in vision pre-training (Tian et al., 2020). To address this, we design and utilize a suite of augmentations.

Our key contributions are:

- **TiRex:** We present TiRex, a pre-trained time series model based on xLSTM, which sets a new state of the art in zero-shot forecasting. It achieves superior performance across standardized benchmarks, improving both short- and long-term forecasting accuracy.
- **Contiguous Patch Masking (CPM):** We propose a novel masking strategy that enhances state-tracking abilities, therefore enabling pre-trained time series models to produce reliable uncertainty estimates over long prediction horizons, effectively addressing autoregressive error accumulation.
- **Data Augmentation Strategies:** We introduce three augmentation techniques for time series model pre-training and demonstrate their effectiveness in enhancing the robustness and overall performance of TiRex.

After introducing the problem setup and a review of related work, the paper is structured as follows: Section 2 introduces TiRex, its architecture, inference strategy, and Contiguous Patch Masking utilized for training. Section 3 describes the proposed training augmentations. Section 4 evaluates TiRex on two standardized real-world benchmarks and examines the impact of the individual components. In Section 5, we discuss limitations of our approach and conclude the paper.

1.1 Problem Setup: Zero-Shot Forecasting

Time series forecasting aims to predict future values of a time series based on its past values. Formally, given a time series (y_1, y_2, \dots, y_T) , with $y_t \in \mathbb{R}$ denoting the value at time t , the forecasting objective is to predict its future horizon $(y_{T+1}, \dots, y_{T+h})$, where h is the forecast horizon’s length. Throughout the paper, we adopt Python-style array notation and denote a contiguous sequence of values by $\mathbf{y}_{1:T} := (y_t)_{t=1}^T = (y_1, y_2, \dots, y_T)$. Probabilistic forecasting extends this setup by

modeling the uncertainty inherent in most time series data. Instead of producing point estimates, the model learns to approximate the conditional distribution over future outcomes:

$$\mathcal{P}(\mathbf{y}_{T+1:T+h} \mid \mathbf{y}_{1:T}). \quad (1)$$

In a zero-shot forecasting setting, the prediction model is pre-trained on a corpus of time series datasets $C = \{D_1, D_2, \dots, D_N\}$, where each D_n , $1 \leq n \leq N$, is a time series dataset, e.g., a set of time series from a particular domain. At inference the model is applied directly to time series of new, unseen dataset, i.e., $\mathbf{y} \in D^{\text{test}}$ and $\mathbf{y} \notin \bigcup_{i=1}^N D_i$, without any fine-tuning or task-specific supervision.

1.2 Related Work

Statistical models such as ARIMA (Box & Jenkins, 1968) and exponential smoothing (Hyndman et al., 2008) are classical approaches in time series forecasting. In the last decades, however, neural network-based models have emerged as effective alternatives: Notable examples include DeepAR (Salinas et al., 2020), based on a LSTM with a mixture density head; N-BEATS (Oreshkin et al., 2019), the first approach that employed a deep block architecture; PatchTST (Nie et al., 2022), a patch-based attention approach; and TFT (Lim et al., 2021), which combines LSTM and transformer components. These models are trained on multiple time series from a single dataset and require retraining when applied to new tasks.

Currently, pre-trained time series models, with the capability of zero-shot generalization across datasets, predominantly adopt different transformer architectures. For instance, Chronos (Ansari et al., 2024a) and Chronos-Bolt (Ansari et al., 2024b) use an encoder-decoder variant. Moirai (Woo et al., 2024) adopts an encoder-only design with a masked modeling objective, and TimesFM (Das et al., 2024) follows a decoder-only causal modeling strategy for autoregressive generation. TabPFN (Hollmann et al., 2025) and its adaptation to time series TabPFN-TS (Hollmann et al., 2025) use a modified transformer encoder and pre-train only on synthetic data. A notable exception is TTM (Ekamparam et al., 2024), since it builds on the MLP-based TSMixer architecture (Chen et al., 2023).

The dominance of transformer architectures echoes their strong in-context learning capabilities (an essential property for zero-shot forecasting) which are known from the language domain (Brown et al., 2020). However, despite their success in language, they often fall short of expectations in time series forecasting. For example, Zeng et al. (2023) show that DLinear, a simple linear model, can outperform transformers in multiple scenarios. Classical models, like LSTMs, are still widely used and remain competitive. While LSTMs are well-suited for time series, they lack strong in-context learning capabilities. Recent advancements in recurrent architectures — such as the xLSTM (Beck et al., 2025) — closed this gap. xLSTM shows promise in task-specific time series applications (Kraus et al., 2024), yet its potential for pre-trained, general-purpose models remains underexplored.

2 TiRex

TiRex utilizes xLSTM as its backbone architecture, and adopts a decoder-only mode, which allows for efficient training. It stacks multiple xLSTM blocks between a lightweight input and output layer. The input layer preprocesses the time series via scaling and patching operations, producing tokens that are subsequently processed by the xLSTM blocks. The output tokens correspond to forecasted patches of the target series and are mapped back to the forecast horizon. For multi-patch forecasting, additional inputs are encoded as missing values. An overview of the architecture is provided in Figure 2 with individual components being described in detail below.

xLSTM Block TiRex adopts the block design proposed by Beck et al. (2025), but substitutes the mLSTM with a sLSTM module as the sequence mixing component. Both module options were introduced in the original publication, but only sLSTM allows for state-tracking (by trading it for reduced memory capacity Beck et al., 2024). Each block comprises a sLSTM module followed by a feed-forward network, with both components preceded by RMSNorm (Zhang & Sennrich, 2019). Additionally, all sLSTM and feedforward layers include residual skip connections. sLSTM supports real recurrence, to enable state-tracking, yet is still efficient in training and inference due to an optimized kernel architecture (Pöppel et al., 2024). TiRex stacks multiple of these blocks, depending on the model size. After the last block, an additional RMSNorm is applied. More details on the general xLSTM architecture are provided in Appendix A.

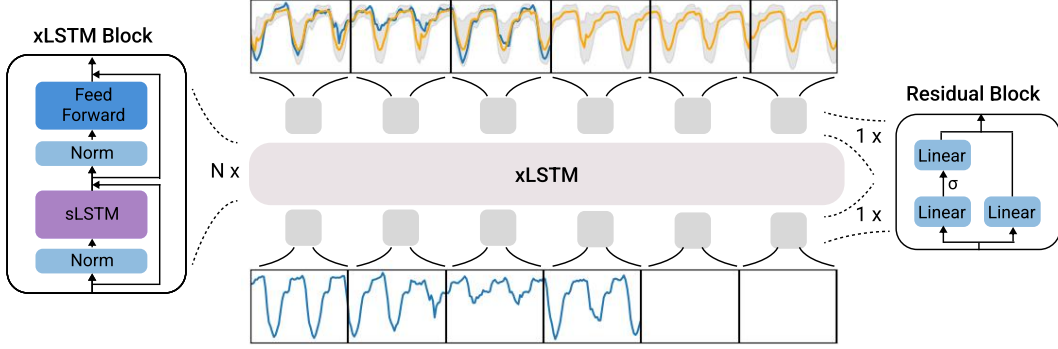


Figure 2: Architecture overview of TiRex. The model comprises two main components: the xLSTM blocks and a residual block in the input and output layers. The illustrated forecast shows the forecasted series is in blue and the forecast of TiRex in orange. During inference, only the last three output windows are of interest.

Input/Output Layer and Loss TiRex is designed to generalize across diverse time series domains, which often exhibit significant variation in scale. To ensure robustness, TiRex applies instance normalization to each time series (Kim et al., 2021). Specifically, z -score normalization is used. That is, $\tilde{y}_{0:T} = \frac{y_{0:T} - \bar{y}_{0:T}}{\sigma_{y_{0:T}}}$, where, \bar{y} and, σ_y denote the mean and standard deviation of the time series sample.

TiRex segments time series into non-overlapping windows, and maps each window to the input space of the xLSTM using a two-layer residual block (He et al., 2016; Srivastava et al., 2015). This patching mechanism is inspired by vision transformers (Dosovitskiy et al., 2020) and was adapted for time series by Nie et al. (2022) and Woo et al. (2024). It reduces the effective sequence length of the xLSTM blocks by a factor defined by the window size. To account for missing values, a binary mask indicating presence or absence is concatenated to the time series values before the residual block. Given an input window of size m_{in} and xLSTM hidden dimension d , the patching block defines a mapping $\mathbb{R}^{2m_{in}} \rightarrow \mathbb{R}^d$. The same residual block is shared across all time windows.

Mirroring the input layer, the decoder’s output tokens are transformed back to the dimensions of the output-patch window using a residual block and subsequently scaled back to the original target space. Hereby, the model outputs provides $|Q|$ quantile values for each time step of the output-patch window, rather than single-point predictions. Hence, the output block defines a mapping $\mathbb{R}^d \rightarrow \mathbb{R}^{m_{out} \times |Q|}$. Specifically, TiRex predicts nine equidistant quantile levels, $Q = \{0.1, 0.2, \dots, 0.9\}$. The model’s parameters are optimized by minimizing the quantile loss. The loss is calculated for each output token, therefore, the loss does not distinguish context and forecast for a training sample, but implicitly “forecast after each input token”. Formally, the loss for an output window, given the true value y_t at time t and its corresponding quantile predictions \hat{y}_t^q for quantile level q is computed as:

$$L = \frac{1}{|Q| m_{out}} \sum_{t=1}^{m_{out}} \sum_{q \in Q} \begin{cases} q (y_t - \hat{y}_t^q) & \text{if } \hat{y}_t^q \leq y_t \\ (1 - q) (\hat{y}_t^q - y_t) & \text{else} \end{cases} . \quad (2)$$

The losses of all output tokens of a training sample are averaged — missing values in the output window are ignored for the loss calculation.

Multi-Patch Horizon Forecasts When the forecast horizon h exceeds the output patch length, multiple future patches must be predicted. We refer to this as multi-patch prediction. Existing pre-trained models (Das et al., 2024; Ansari et al., 2024b) typically address multi-patch prediction via autoregressive generation, using point estimates (say, mean or median) of previous outputs as inputs for subsequent patches. However, this approach reinitializes the probabilistic forecast at each step, disrupting the propagation of uncertainty. In contrast, TiRex treats future inputs as missing values, allowing the internal memory to propagate both predictive state and uncertainty across patches. This results in more coherent probabilistic and overall better forecasts, as our quantitative and qualitative experiments show (Section 4 and Figure 1).

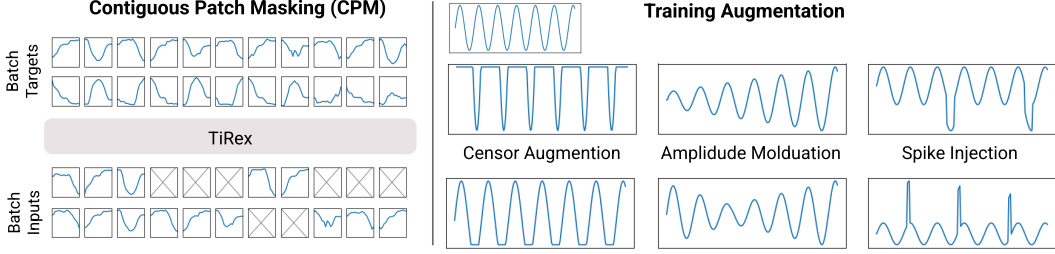


Figure 3: Illustration of Contiguous Patch Masking and the different training augmentations.

2.1 Contiguous Patch Masking

To facilitate the stable multi-patch prediction capability of TiRex, we propose Contiguous Patch Masking (CPM), illustrated in Figure 3. CPM randomly masks full and consecutive patches in pre-training. Such a masked patch is represented as “missing values” in the model input, hence corresponds to the structure of the input when multi-patch forecasts are used in the inference. The procedure is as follows: For each training sample, we first uniformly sample the amount of consecutive patches $c_{\text{mask}} \sim U(1, c_{\text{mask}}^{\text{max}})$ and the masking probability $p_{\text{mask}} \sim U(0, p_{\text{mask}}^{\text{max}})$. Afterwards, we mask the time series: For a time series of length T we sample a binary mask of length $\lfloor \frac{T}{c_{\text{mask}} m_{\text{out}}} \rfloor$ with Bernoulli probability p_{mask} and repeat each element $c_{\text{mask}} \cdot m_{\text{out}}$ so that the mask has a length of T too. Note that when neighboring elements are masked, the actual maximum of consecutive masked patches can be greater than $c_{\text{mask}}^{\text{max}}$. Further, while CPM incorporates elements from BERT-style (Devlin et al., 2019) masked-modeling, our training is still more similar to the typical causal-style masking of decoder-only approaches (Radford et al., 2018) since the target is shifted and the information flow is uni-directional. Appendix D.3 provides a sensitivity analysis of the parameters $p_{\text{mask}}^{\text{max}}$ and $c_{\text{mask}}^{\text{max}}$.

3 Data Augmentation

To facilitate more diverse time series patterns and enhance the model’s exposure to a wider range of potentially relevant dynamics, we propose three augmentations for pre-training. This is inspired by the successful application of augmentation techniques in pre-training of other modalities, e.g., vision (Tian et al., 2020). The employed augmentations, illustrated in Figure 3, are: (1) *Amplitude Modulation*, which introduces trends and change points in the scale of the time series. Formally, a time series \mathbf{y} is transformed by $y'_t = y_t \cdot a_t$, where a_t follows a linear trend (potentially with change points). (2) *Censor Augmentation*, which censors values within the time series at a random threshold. The augmented respective series is computed by $y'_t = \max/\min(y_t, c)$, The censor threshold c is sampled by uniformly drawing a quantile from the empirical distribution of the signal. (3) *Spike Injection*, which adds short, periodic spike signals to the time series. The augmented time series is computed by $y'_t = y_t + s_t$, where s_t represents the added spike signals. The shape of each spike is defined by a kernel, which can be a tophat, a radial basis function (RBF), or a linear kernel. The periodicity and the specific parameters of the kernel (e.g., width, height for tophat; center, variance for RBF) are sampled from predefined distributions for each sample. The augmentations are applied with a probability of 0.5 for amplitude modulation and censor augmentation and 0.05 for spike augmentation. Appendix B provides a more detailed description of the augmentation procedures.

4 Experiments

This section outlines the experimental setup, including training procedures, evaluation benchmarks, and comparison models. We further report the main results demonstrating the effectiveness of TiRex in general (Section 4.1) and the specific components — the xLSTM backbone, Contiguous Patch Masking, and the proposed augmentations (Section 4.2). Full experimental details are provided in Appendix C, while extended results are presented in Appendix D.

TiRex Training Our training data comprises three components: (1) We utilize the training datasets from Chronos (Ansari et al., 2024a), and adopt their TSMixup procedure to augment this data. (2)

We enrich our training data with synthetic time series data generated through a procedure closely inspired by KernelSynth (Ansari et al., 2024a). (3) We add parts of the pre-training dataset proposed by GiftEval (Aksu et al., 2024). In total, our training dataset encompasses 47.5 million time series samples. Details regarding the specific datasets employed, as well as the implementation of the TSMixup and synthetic data generation procedures, can be found in Appendix C.2. During training, we augment the samples with the proposed training augmentations and apply Contiguous Patch Masking as described in Section 3. We train TiRex with a context length of 2048 and a window size of 32 for input and output patches.

Evaluation Benchmarks We evaluate TiRex on two standardized benchmarks with public leaderboards: (1) the Chronos Zero-Shot Benchmark¹, comprising 27 diverse datasets, each in one evaluation setting, primarily for short-term horizons (Ansari et al., 2024a), and (2) the GiftEval benchmark² (Aksu et al., 2024), which includes 24 datasets that are evaluated in different settings, and covers short-, medium-, and long-term horizons, as well as different frequencies — in sum 97 evaluation settings. The training data of TiRex has no overlap with this data, hence TiRex operates in zero-shot. We denote this benchmark as *Chronos-ZS benchmark*. To also ensure zero-shot conditions on the GiftEval benchmark, we exclude 16 of the 97 evaluation settings, which overlap with our training data, and denote this benchmark as *GiftEval-ZS benchmark*; complete results for GiftEval are reported in Appendix D.1. We note that all Chronos models do have the same overlap as TiRex; TimesFM, and Moirai have additional overlapping datasets and additionally also have overlaps with the Chronos-ZS benchmark.

The evaluation follows the respective benchmark protocols using mean absolute scaled error (MASE) for point forecast performance and the continuous ranked probability score (CRPS) for probabilistic forecast performance. Practically, the CRPS is approximated by the mean weighted quantile loss (WQL) over nine quantiles: 0.1 to 0.9 in increments of 0.1³. Aggregated performance is computed by normalizing each evaluation setting’s score by that of a seasonal naive baseline, followed by the geometric mean across evaluation settings. Additionally, the average rank across evaluation settings is reported to ensure robustness against outlier performance.

Compared Models We compare TiRex against a broad set of state-of-the-art models, including zero-shot pre-trained models and task-specific models. The zero-shot models include Chronos and Chronos-Bolt (Ansari et al., 2024a,b), TimesFM (v1.0, v2.0) (Das et al., 2024), Moirai 1.1 (Woo et al., 2024), TabPFN-TS (Hollmann et al., 2025), and Tiny Time Mixer (TTM) (Ekambaram et al., 2024). The task-specific models are PatchTST (Nie et al., 2022), TFT (Lim et al., 2021), DLinear (Zeng et al., 2023), DeepAR (Salinas et al., 2020), and N-BEATS (Oreshkin et al., 2019). These models are trained individually on each dataset. Hence, they do not operate in ‘zero-shot’ and only provide an asymmetric comparison. Reporting their result is useful to contextualize the current strengths and limitations of zero-shot approaches. We report the results of the public leaderboards if available and replicate the outcomes of pre-trained models within our evaluation pipeline to ensure validity.

4.1 Zero-Shot Forecasting

GiftEval-ZS Benchmark In this benchmark TiRex consistently outperforms all competing methods across both short- and long-term forecasting tasks (Figure 4). In terms of CRPS, TiRex achieves a score of 0.411 (with standard deviation over training with 6 seeds of ± 0.002), notably surpassing the next best zero-shot models (0.459, 0.463, 0.481). This performance gap is also reflected in the average rank, where TiRex shows a substantial lead over the second-best model, while the three models that following in the ranking (TimesFM-2.0, TabPFN, and Chronos-Bolt-Base) achieve very similar scores among themselves. Importantly, while other models tend to peak either in short- (e.g., Chronos-Bolt) or long-term (e.g., TabPFN-TS) forecasting, TiRex is the only model to excel simultaneously at both. Moreover, TiRex attains these results with significantly fewer parameters (35M) compared to Chronos-Bolt-Base (200M) and TimesFM-2.0 (500M). The advantage is most pronounced in long-term forecasting, where TiRex becomes the first zero-shot model to surpass the performance of PatchTST and TFT.

¹[HuggingFace.co/spaces/autogluon/fev-leaderboard](https://huggingface.co/spaces/autogluon/fev-leaderboard)

²[HuggingFace.co/spaces/Salesforce/GIFT-Eval](https://huggingface.co/spaces/Salesforce/GIFT-Eval)

³In the Chronos-ZS benchmark, the mean weighted quantile loss (WQL) is used directly, hence, essentially both benchmarks evaluate on the same metric

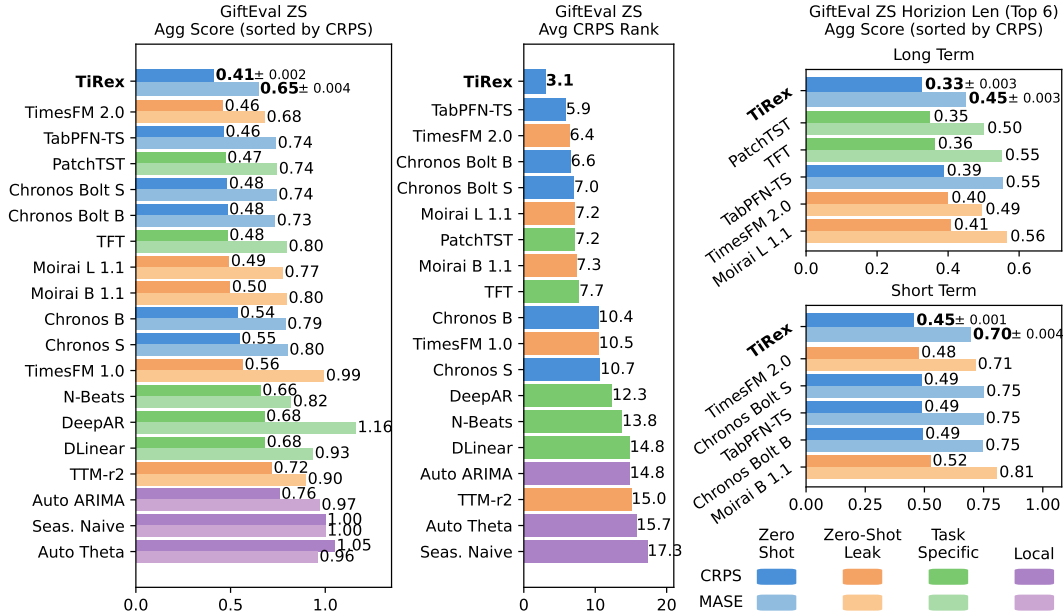


Figure 4: Results of the GiftEval-ZS benchmark: Aggregated scores of the overall benchmark and the short- and long-term performances. Additionally, the average rank in terms of CRPS, as in the public leaderboard, is presented. Lower values are better. “Zero-shot Leak” refers to models which are partly trained on the benchmark datasets (Overlap: Moirai 19%, TimesFM 10%, TTM: 16%). We trained TiRex with 6 different seeds and report the observed standard deviation in the plot.

Chronos-ZS Benchmark The main results on the Chronos-ZS benchmark exhibit similar performance patterns to those observed on the GiftEval-ZS benchmark (Figure 5). TiRex again achieves the best results in terms of WQL score and rank. In the MASE score TiRex has second best score, closely behind TabPFN-TS. Notably, Moirai performs substantially better on the Chronos-ZS benchmark (compared to the GiftEval-ZS benchmark). However, this improvement is likely due to the substantial overlap of 82% between its pre-training data and the Chronos-ZS test set. These results highlight the robustness of TiRex in zero-shot generalization. The full results, including task-specific models are presented in Appendix D.2.

Qualitative Analysis We also qualitatively analyzed the predictions of TiRex and compared them against current state-of-the-art methods. Beyond its generally higher forecasting accuracy, the analysis shows that TiRex demonstrates robust multi-patch prediction capabilities, maintaining coherent uncertainty estimates across different forecast horizons — and more accurately forecasts short periodic spikes, which are often missed or smoothed out by other models (Figure 1 and Appendix D.4). We hypothesize that these improvements mainly stem from (i) the effective multi-patch forecasting due to CPM, (ii) the sLSTM architecture that provides state-tracking for uncertainty propagation and strong periodicity modeling, and (iii) the spike augmentation strategy enhancing the model’s sensitivity to rare, sharp events during training.

Inference Speed & Memory Apart from the forecasting performance, we analyze the GPU memory consumption and inference runtime across all models. Specifically, we evaluate samples with a context length of 2048 and a prediction length of 32 over multiple batch sizes. As expected, given TiRex substantially smaller size compared to the next best models (TimesFM-2.0 and Chronos-Bolt-Base), TiRex requires significantly less GPU memory and achieves faster inference speeds. Specifically, TiRex is over 11× faster than TimesFM-2.0, over 4× faster than Chronos-Bolt Base, and over 2176× faster than TabPFN-TS. Furthermore, TiRex even outperforms Chronos-Bolt Small, a similarly sized transformer-based architecture for larger batch sizes. The differences in maximum GPU memory consumption follow a similar order.

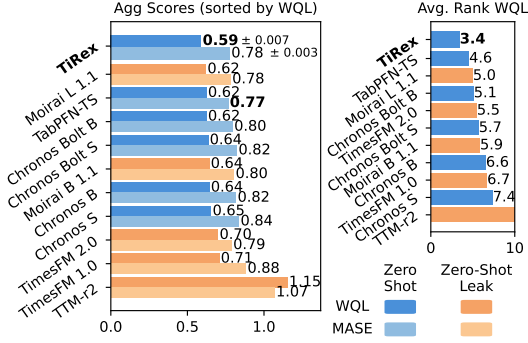


Figure 5: Results of pre-trained model on the Chronos-ZS benchmark. The aggregated MASE and WQL scores, and the average rank in terms of WQL is shown. Lower values are better. “Zero-shot Leak” refers to models which are partly trained on the benchmark datasets (Overlap: Moirai 82%, TimesFM 15%, TTM: 11%).

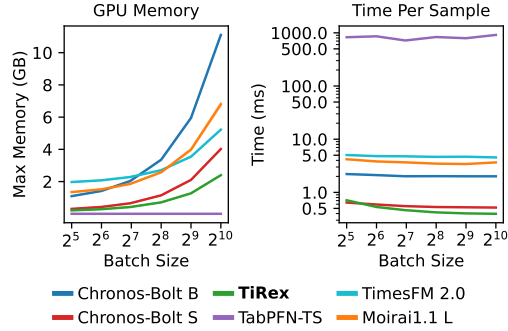


Figure 6: Inference efficiency of the best-performing pre-trained models. Left: Relation between GPU memory and batch size. Right: Inference time per sample and batch size.

4.2 Ablations

We conduct ablation studies to analyze the impact of key components in TiRex. Specifically, this section focuses on Contiguous Patch Masking (CPM), the proposed data augmentations, and the xLSTM backbone architecture.

Contiguous Patch Masking and Multi-Patch-Inference We analyze the effectiveness of the proposed Contiguous Patch Masking (CPM) procedure by comparing three configurations: (1) standard decoder-only training with autoregressive inference — this setting is similar e.g., to TimesFM; (2) training with a naive multiple-patch procedure where we place the “rollout” always at the end of the sequence; and (3) training with CPM. Configurations (2) and (3) use the same inference procedure with masked tokens for multi-step forecasting, whereas (1) relies on patch-wise autoregressive decoding. As shown in Table 1 only CPM enables strong long-term performance without degrading short-term performance. In contrast, naive multi-patch training diminishes the short-term forecasting performance, and standard next token training combined with autoregressive inference harms the long-term forecasting performance. These findings suggest that CPM is essential for training and inference behaviors under multi-patch prediction.

Augmentation To assess the impact of our augmentations, we trained our model excluding each augmentation and with no augmentations at all. The results, detailed in Table 1, indicate that including the augmentations is beneficial, i.e., improves the performance of the model. Performance consistently decreased in at least one benchmark metric when any single augmentation was removed. The most substantial decline occurs when no augmentations were applied. This underscores the effectiveness of each augmentation and their combined positive impact on the model’s generalization capabilities. Appendix D.3 provides a sensitivity analysis in terms of application probability.

Backbone To assess the architectural choice of xLSTM with sLSTM modules, we replace it with mLSTM (Beck et al., 2024) and transformer blocks (Touvron et al., 2023) while keeping the patching and training procedure unchanged. For the transformer variant, rotary positional embeddings (Su et al., 2024) are added to mitigate the absence of inherent positional information, due to their permutation-invariance property. We also analyze mLSTM and sLSTM mix architectures as proposed in the original xLSTM paper. We denote xLSTM[i:j] for an architecture where i sLSTM blocks are combined with j mLSTM blocks. Additionally, we ablate our overall architecture by comparing it to a Chronos-Bolt architecture (Base and Small) that we train with our training procedure, using the same datasets and augmentations as for TiRex. Table 1 summarizes the results. TiRex with only sLSTM blocks yields the best performance, especially on long-term forecasts. We hypothesize that this is because its explicit state-tracking capabilities (Beck et al., 2024), which might facilitate uncertainty propagation and enable accurate modeling of periodic temporal structures over extended

horizons. Using only mLSTM performs worst. However, switching just one of these blocks back to a sLSTM improves the results close to the sLSTM-only architecture of TiRex. The comparison to a Chronos Bolt architecture, which is consistently outperformed by TiRex, highlights that our overall architecture is critical to achieve good performance on both long and short-term forecasting. A more detailed comparison to the Chronos Bolt architecture is presented in Appendix D.3.

Table 1: Ablation study of individual components. The top two rows report the mean and standard deviation of TiRex over six runs with different random seeds. For the ablation variants, results that degrade performance by more than $3\times$ the standard deviation relative to TiRex are underlined. Columns correspond to evaluation settings: GiftEval-ZS benchmark (overall, short-term, and long-term) and Chronos-ZS benchmark. Lower values indicate better performance.

	Benchmark	Gift-ZS Overall CRPS MASE	Gift-ZS Long CRPS MASE	Gift-ZS Short CRPS MASE	Chronos-ZS WQL MASE
	TiRex	0.411 0.647	0.325 0.45	0.455 0.696	0.592 0.776
	± 6 seeds	0.002 0.004	0.003 0.003	0.001 0.004	0.007 0.003
CPM	naïve multi-patch	<u>0.424</u> <u>0.662</u>	<u>0.335</u> <u>0.460</u>	<u>0.475</u> <u>0.718</u>	<u>0.650</u> <u>0.817</u>
	w/o multi-patch	<u>0.445</u> <u>0.704</u>	<u>0.370</u> <u>0.518</u>	<u>0.471</u> <u>0.719</u>	0.589 0.777
Augment	w/o any	<u>0.430</u> <u>0.682</u>	<u>0.339</u> <u>0.478</u>	<u>0.473</u> <u>0.722</u>	<u>0.623</u> <u>0.800</u>
	w/o censor	0.417 0.652	<u>0.336</u> 0.457	0.458 0.699	0.595 0.767
	w/o spike	0.415 <u>0.660</u>	0.328 0.459	<u>0.462</u> <u>0.710</u>	0.591 0.773
	w/o amplitude modulation	0.409 0.644	0.323 0.448	0.455 0.694	<u>0.618</u> <u>0.798</u>
Backbone	Transformer	<u>0.422</u> <u>0.662</u>	<u>0.342</u> <u>0.472</u>	<u>0.461</u> 0.702	0.597 0.768
	mLSTM	<u>0.457</u> <u>0.718</u>	<u>0.430</u> <u>0.589</u>	0.456 0.699	0.588 0.775
	xLSTM[1:11]	0.414 0.652	0.330 0.456	0.455 0.698	<u>0.631</u> <u>0.807</u>
	xLSTM[1:5]	0.412 0.651	0.330 <u>0.460</u>	0.450 0.693	0.611 <u>0.791</u>
	Chronos Bolt S	<u>0.456</u> <u>0.676</u>	<u>0.413</u> <u>0.498</u>	<u>0.463</u> 0.705	0.609 <u>0.791</u>
	Chronos Bolt B	<u>0.454</u> <u>0.670</u>	<u>0.418</u> <u>0.493</u>	0.458 0.701	<u>0.627</u> <u>0.807</u>

5 Conclusion

This work introduces TiRex, a pre-trained time series forecasting model based on xLSTM. To fully unlock the state-tracking capabilities of xLSTM, we further propose Contiguous Patch Masking, a training-time masking strategy tailored for in-context learning. Contiguous Patch Masking is a crucial component in our modeling pipeline, since it enables strong long-term forecasting performance without sacrificing short-term capabilities. TiRex establishes a new state-of-the-art in zero-shot forecasting, outperforming prior methods on both short- and long-term horizons across the Chronos-ZS and GiftEval benchmarks. Our ablation studies highlight the individual contributions of each component to overall performance.

Limitations & Future Work Like most pre-trained forecasting models, TiRex focuses on univariate time series. Although modeling multivariate series as independent univariate signals often performs well — as reflected in the GiftEval results and, for example, shown in Nie et al. (2022) — future work could incorporate multivariate data, for example in the form of extended contexts or modified input layers. Due to computational constraints, we did not extensively tune hyperparameters and only conducted a sensitivity analysis on key parameters. Future work should explore more comprehensive tuning for additional performance gains.

Acknowledgments and Disclosure of Funding

We thank Maximilian Beck and Korbinian Pöppel for the discussions and advice in regard to xLSTM. The ELLIS Unit Linz, the LIT AI Lab, and the Institute for Machine Learning are supported by the Federal State Upper Austria.

References

- Aksu, T., Woo, G., Liu, J., Liu, X., Liu, C., Savarese, S., Xiong, C., and Sahoo, D. GIFT-eval: A benchmark for general time series forecasting model evaluation. In *NeurIPS Workshop on Time Series in the Age of Large Models*, 2024.
- Ansari, A. F., Stella, L., Turkmen, A. C., Zhang, X., Mercado, P., Shen, H., Shchur, O., Rangapuram, S. S., Arango, S. P., Kapoor, S., Zschiegner, J., Maddix, D. C., Wang, H., Mahoney, M. W., Torkkola, K., Wilson, A. G., Bohlke-Schneider, M., and Wang, B. Chronos: Learning the Language of Time Series. *Transactions on Machine Learning Research*, May 2024a. ISSN 2835-8856.
- Ansari, A. F., Turkmen, C., Shchur, O., and Stella, L. Fast and accurate zero-shot forecasting with Chronos-Bolt and AutoGluon, December 2024b. URL <https://aws.amazon.com/blogs/machine-learning/fast-and-accurate-zero-shot-forecasting-with-chronos-bolt-and-autogluon/>.
- Beck, M., Pöppel, K., Spanring, M., Auer, A., Prudnikova, O., Kopp, M. K., Klambauer, G., Brandstetter, J., and Hochreiter, S. xLSTM: Extended Long Short-Term Memory. In *The Thirty-eighth Annual Conference on Neural Information Processing Systems*, November 2024.
- Beck, M., Pöppel, K., Lippe, P., Kurle, R., Blies, P. M., Klambauer, G., Böck, S., and Hochreiter, S. xLSTM 7B: A Recurrent LLM for Fast and Efficient Inference, 2025.
- Box, G. E. P. and Jenkins, G. M. Some Recent Advances in Forecasting and Control. *Journal of the Royal Statistical Society Series C*, 17(2):91–109, 1968.
- Brown, T., Mann, B., Ryder, N., Subbiah, M., Kaplan, J. D., Dhariwal, P., Neelakantan, A., Shyam, P., Sastry, G., Askell, A., et al. Language models are few-shot learners. *Advances in neural information processing systems*, 33:1877–1901, 2020.
- Chen, S.-A., Li, C.-L., Yoder, N., Arik, S. O., and Pfister, T. TSMixer: An All-MLP Architecture for Time Series Forecasting. *ArXiv*, 2303.06053, 2023.
- Das, A., Kong, W., Sen, R., and Zhou, Y. A decoder-only foundation model for time-series forecasting. In *Proceedings of the 41st International Conference on Machine Learning*, pp. 10148–10167. PMLR, July 2024.
- Delétang, G., Ruoss, A., Grau-Moya, J., Genewein, T., Wenliang, L. K., Catt, E., Cundy, C., Hutter, M., Legg, S., Veness, J., and Ortega, P. A. Neural networks and the Chomsky hierarchy. In *International Conference on Learning Representations (ICLR)*, volume 11, 2023.
- Devlin, J., Chang, M.-W., Lee, K., and Toutanova, K. Bert: Pre-training of deep bidirectional transformers for language understanding. In *Proceedings of the 2019 conference of the North American chapter of the association for computational linguistics: human language technologies, volume 1 (long and short papers)*, pp. 4171–4186, 2019.
- Dosovitskiy, A., Beyer, L., Kolesnikov, A., Weissenborn, D., Zhai, X., Unterthiner, T., Dehghani, M., Minderer, M., Heigold, G., Gelly, S., Uszkoreit, J., and Housley, N. An Image is Worth 16x16 Words: Transformers for Image Recognition at Scale. In *International Conference on Learning Representations*, October 2020.
- Ekambaram, V., Jati, A., Dayama, P., Mukherjee, S., Nguyen, N. H., Gifford, W. M., Reddy, C., and Kalagnanam, J. Tiny Time Mixers (TTMs): Fast Pre-trained Models for Enhanced Zero/Few-Shot Forecasting of Multivariate Time Series. *ArXiv*, 2401.03955, 2024.
- Gardner, J. R., Pleiss, G., Bindel, D., Weinberger, K. Q., and Wilson, A. G. Gpytorch: Blackbox matrix-matrix gaussian process inference with gpu acceleration. In *Advances in Neural Information Processing Systems*, 2018.
- He, K., Zhang, X., Ren, S., and Sun, J. Deep residual learning for image recognition. In *2016 IEEE Conference on Computer Vision and Pattern Recognition (CVPR)*, pp. 770–778, 2016. doi: 10.1109/CVPR.2016.90.

- Hochreiter, S. Untersuchungen zu dynamischen neuronalen Netzen. Diploma thesis, Institut für Informatik, Lehrstuhl Prof. Brauer, Technische Universität München, 1991.
- Hochreiter, S. and Schmidhuber, J. Long short-term memory. *Neural Comput.*, 9(8):1735–1780, 1997.
- Hochreiter, S., Younger, A. S., and Conwell, P. R. Learning to learn using gradient descent. In Dorffner, G., Bischof, H., and Hornik, K. (eds.), *Proc. Int. Conf. on Artificial Neural Networks (ICANN 2001)*, pp. 87–94. Springer, 2001.
- Hollmann, N., Müller, S., Purucker, L., Krishnakumar, A., Körfer, M., Hoo, S. B., Schirrmeyer, R. T., and Hutter, F. Accurate predictions on small data with a tabular foundation model. *Nature*, 637(8045):319–326, January 2025. ISSN 1476-4687. doi: 10.1038/s41586-024-08328-6.
- Hyndman, R., Koehler, A., Ord, K., and Snyder, R. *Forecasting with Exponential Smoothing*. Springer Series in Statistics. Springer, Berlin, Heidelberg, 2008. ISBN 978-3-540-71916-8 978-3-540-71918-2. doi: 10.1007/978-3-540-71918-2.
- Kim, T., Kim, J., Tae, Y., Park, C., Choi, J.-H., and Choo, J. Reversible Instance Normalization for Accurate Time-Series Forecasting against Distribution Shift. In *International Conference on Learning Representations*, October 2021.
- Kraus, M., Divo, F., Dhami, D. S., and Kersting, K. xlstm-mixer: Multivariate time series forecasting by mixing via scalar memories. *ArXiv*, 2410.16928, 2024.
- Lim, B., Arik, S. Ö., Loeff, N., and Pfister, T. Temporal Fusion Transformers for interpretable multi-horizon time series forecasting. *International Journal of Forecasting*, 37(4):1748–1764, October 2021. ISSN 0169-2070. doi: 10.1016/j.ijforecast.2021.03.012.
- Merrill, W. and Sabharwal, A. The parallelism tradeoff: Limitations of log-precision transformers. *Transactions of the Association for Computational Linguistics*, 11:531–545, 2023. doi: 10.1162/tacl_a_00562.
- Merrill, W., Petty, J., and Sabharwal, A. The illusion of state in state-space models. *ArXiv*, 2404.08819, 2024.
- Nearing, G., Cohen, D., Dube, V., Gauch, M., Gilon, O., Harrigan, S., Hassidim, A., Klotz, D., Kratzert, F., Metzger, A., et al. Global prediction of extreme floods in ungauged watersheds. *Nature*, 627(8004):559–563, 2024.
- Nie, Y., Nguyen, N. H., Sinthong, P., and Kalagnanam, J. A Time Series is Worth 64 Words: Long-term Forecasting with Transformers. In *The Eleventh International Conference on Learning Representations*, September 2022.
- Oreshkin, B. N., Carpov, D., Chapados, N., and Bengio, Y. N-BEATS: Neural basis expansion analysis for interpretable time series forecasting. In *International Conference on Learning Representations*, September 2019.
- Peng, B., Alcaide, E., Anthony, Q., Albalak, A., Arcadinho, S., Biderman, S., Cao, H., Cheng, X., Chung, M., Grella, M., et al. Rwkv: Reinventing rnns for the transformer era. *ArXiv*, 2305.13048, 2023.
- Pöppel, K., Beck, M., and Hochreiter, S. FlashRNN: I/O-Aware Optimization of Traditional RNNs on modern hardware. In *International Conference on Learning Representations*, October 2024.
- Radford, A., Narasimhan, K., Salimans, T., Sutskever, I., et al. Improving language understanding by generative pre-training. 2018.
- Salinas, D., Flunkert, V., Gasthaus, J., and Januschowski, T. DeepAR: Probabilistic forecasting with autoregressive recurrent networks. *International Journal of Forecasting*, 36(3):1181–1191, July 2020. ISSN 0169-2070. doi: 10.1016/j.ijforecast.2019.07.001.
- Srivastava, R. K., Greff, K., and Schmidhuber, J. Training Very Deep Networks. *ArXiv*, 1507.06228, 2015.

- Su, J., Ahmed, M., Lu, Y., Pan, S., Bo, W., and Liu, Y. Roformer: Enhanced transformer with rotary position embedding. *Neurocomputing*, 568:127063, 2024.
- Tian, Y., Sun, C., Poole, B., Krishnan, D., Schmid, C., and Isola, P. What makes for good views for contrastive learning? *Advances in neural information processing systems*, 33:6827–6839, 2020.
- Touvron, H., Lavril, T., Izacard, G., Martinet, X., Lachaux, M.-A., Lacroix, T., Rozière, B., Goyal, N., Hambro, E., Azhar, F., Rodriguez, A., Joulin, A., Grave, E., and Lample, G. Llama: Open and efficient foundation language models. *ArXiv*, 2302.13971, 2023.
- Vaswani, A., Shazeer, N., Parmar, N., Uszkoreit, J., Jones, L., Gomez, A. N., Kaiser, L., and Polosukhin, I. Attention is All you Need. In *Advances in Neural Information Processing Systems*, volume 30. Curran Associates, Inc., 2017.
- Woo, G., Liu, C., Kumar, A., Xiong, C., Savarese, S., and Sahoo, D. Unified Training of Universal Time Series Forecasting Transformers. In *Forty-First International Conference on Machine Learning*, June 2024.
- Zeng, A., Chen, M., Zhang, L., and Xu, Q. Are transformers effective for time series forecasting? In *Proceedings of the Thirty-Seventh AAAI Conference on Artificial Intelligence and Thirty-Fifth Conference on Innovative Applications of Artificial Intelligence and Thirteenth Symposium on Educational Advances in Artificial Intelligence*, volume 37 of AAAI'23/IAAI'23/EAAI'23, pp. 11121–11128. AAAI Press, February 2023. ISBN 978-1-57735-880-0. doi: 10.1609/aaai.v37i9.26317.
- Zhang, B. and Sennrich, R. Root mean square layer normalization. *Advances in Neural Information Processing Systems*, 32, 2019.

Appendix

Table of Contents

A	xLSTM	13
B	Data Augmentation	15
C	Experiment Details	17
C.1	Model and Training Hyperparameter	17
C.2	Pre-Training Data Corpus	17
C.3	Benchmarks and Metrics	20
C.4	Computation & Hardware	21
D	Extended Results	24
D.1	Full GiftEval leaderboard	24
D.2	Zero-Shot Forecasting	24
D.3	Ablations	28
D.4	Additional qualitative examples	30
D.5	Finetuned-Forecasting	30
E	Societal Impact	30
F	Code	30

A xLSTM

TiRex utilizes xLSTM (Beck et al., 2024) as its backbone architecture. xLSTM extends the classical LSTM (Hochreiter, 1991; Hochreiter & Schmidhuber, 1997) by incorporating modern design principles to improve its scalability, parallelization, and in-context modeling capabilities.

xLSTM introduces two cell types: the matrix LSTM (mLSTM) and the scalar LSTM (sLSTM). The mLSTM is designed to increase memory capacity through a matrix-based memory representation, and enables efficient parallel computation. In contrast, the sLSTM preserves a true recurrent pathway as in the original LSTM, enabling strong state-tracking capabilities (Beck et al., 2024). The recurrent pathway makes LSTM more expressive than State Space Models (SSMs), parallelizable RNNs like RWKV, and transformers (Merrill & Sabharwal, 2023; Merrill et al., 2024; Delétang et al., 2023). Figure 7 illustrates the respective expressivity hierarchies. Delétang et al. (2023) demonstrate on synthetic language tasks that this state-tracking capability of LSTMs yields empirical advantages. Beck et al. (2024) show that sLSTM retains these advantages. sLSTM employs a multi-head strategy along the recurrent pathway to improve efficiency.

TiRex exclusively employs sLSTM cells. Given a sequence of T embedded input patches $\mathbf{X}_{1:T} = (\mathbf{x}_1, \mathbf{x}_2, \dots, \mathbf{x}_T) \in \mathbb{R}^{d \times T}$, the forward computation of an sLSTM cells for a given time step is defined as follows:

$$\mathbf{c}_t = \mathbf{f}_t \odot \mathbf{c}_{t-1} + \mathbf{i}_t \odot \mathbf{z}_t, \quad \text{cell state} \quad (3)$$

$$\mathbf{n}_t = \mathbf{f}_t \odot \mathbf{n}_{t-1} + \mathbf{i}_t, \quad \text{normalizer state} \quad (4)$$

$$\mathbf{h}_t = \mathbf{o}_t \odot \tilde{\mathbf{h}}_t, \quad \tilde{\mathbf{h}}_t = \mathbf{c}_t \odot \mathbf{n}_t^{-1} \quad \text{hidden state} \quad (5)$$

$$\mathbf{z}_t = \varphi(\tilde{\mathbf{z}}_t), \quad \tilde{\mathbf{z}}_t = \mathbf{W}_z \mathbf{x}_t + \mathbf{R}_z \mathbf{h}_{t-1} + \mathbf{b}_z \quad \text{cell input} \quad (6)$$

$$\mathbf{i}_t = \exp(\tilde{\mathbf{i}}_t), \quad \tilde{\mathbf{i}}_t = \mathbf{W}_i \mathbf{x}_t + \mathbf{R}_i \mathbf{h}_{t-1} + \mathbf{b}_i \quad \text{input gate} \quad (7)$$

$$\mathbf{f}_t = \exp(\tilde{\mathbf{f}}_t), \quad \tilde{\mathbf{f}}_t = \mathbf{W}_f \mathbf{x}_t + \mathbf{R}_f \mathbf{h}_{t-1} + \mathbf{b}_f \quad \text{forget gate} \quad (8)$$

$$\mathbf{o}_t = \sigma(\tilde{\mathbf{o}}_t), \quad \tilde{\mathbf{o}}_t = \mathbf{W}_o \mathbf{x}_t + \mathbf{R}_o \mathbf{h}_{t-1} + \mathbf{b}_o \quad \text{output gate,} \quad (9)$$

where $\mathbf{h}_t \in \mathbb{R}^d$ denotes the hidden state, $\mathbf{c}_t \in \mathbb{R}^d$ denotes the cell states and, $\mathbf{n}_t \in \mathbb{R}^d$ denotes a normalizer state. Further, $\mathbf{i}_t, \mathbf{o}_t, \mathbf{f}_t \in \mathbb{R}^d$ are the input, output and forget gate, respectively, $\mathbf{W}_z, \mathbf{W}_i, \mathbf{W}_f, \mathbf{W}_o \in \mathbb{R}^{d \times D}$, $\mathbf{R}_z, \mathbf{R}_i, \mathbf{R}_f, \mathbf{R}_o \in \mathbb{R}^{d \times d}$, and $\mathbf{b}_z, \mathbf{b}_i, \mathbf{b}_f, \mathbf{b}_o \in \mathbb{R}^d$ are trainable weight matrices and biases. The matrices $\mathbf{R}_z, \mathbf{R}_i, \mathbf{R}_f, \mathbf{R}_o$ are block-diagonal, where each block represents one head. This way, the parameters reduce to $d^2/(N_h)$, where N_h is the number of heads, limiting the cell interactions to individual heads. The input-, output-, and forget-gates are activated by exponential (exp) or sigmoid functions (σ); The cell inputs use a hyperbolic tangent function (φ).

To enable deep modeling, xLSTM organizes its recurrent layers into blocks that combine sLSTM and/or mLSTM layers with additional architectural components. Specifically, TiRex uses the block structure from Beck et al. (2025) that consists of

1. an sLSTM module
2. a feed forward network
3. residual connections around each subcomponent,
4. and pre-normalization layers (RMSNorm)

This block architecture is illustrated in Figure 2 and allows for the training of deep networks. To achieve scalability, xLSTM employs custom CUDA kernels that enable high-throughput training and inference on modern hardware (Pöppel et al., 2024).

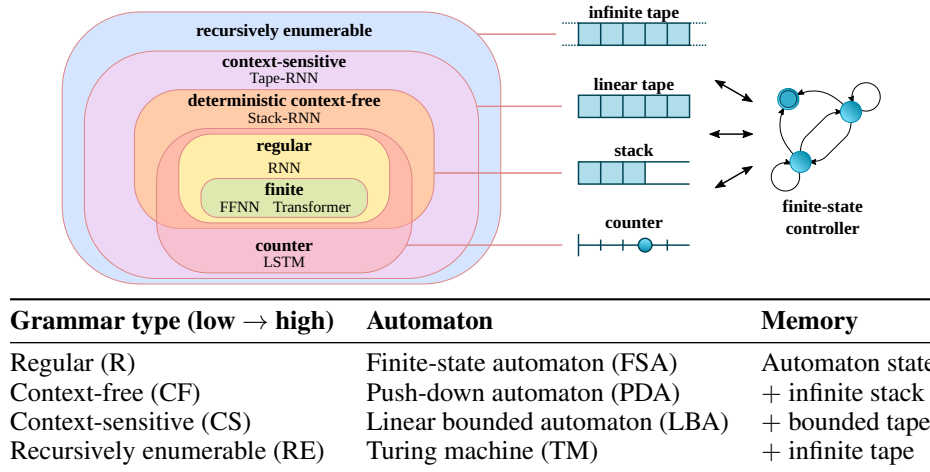


Figure 7: Formal language classes and their correspondence with neural network architectures and k -counter machines that have a counting mechanism (from: Delétang et al., 2023).

B Data Augmentation

This section details the time series augmentations proposed and used for pre-training TiRex.

Amplitude Modulation This augmentation introduces scale trends and change points into the time series by multiplying the signal with a piecewise linear trend. The modulation trend is generated by sampling change points and interpolating amplitudes between them. See Algorithm 1.

Censor Augmentation This augmentation censors (clips) the input signal either from below or above, depending on a randomly sampled direction. The clipping threshold is determined by drawing a quantile uniformly from the empirical distribution of the signal. See Algorithm 2.

Spike Injection This augmentation injects a structured additive signal in the form of sparse, periodic spikes. First, a periodic pattern is sampled, which is then tiled across the time axis with a sampled periodicity. Each spike label in the pattern is mapped to a kernel (selected from a fixed set) with randomized parameters that control its shape and magnitude. The final augmentation is the sum of all such kernel evaluations added to the original signal. See Algorithm 3. The spike kernel types and their parameter ranges are defined in Table 2, while the available temporal patterns and their sampling probabilities are described in Table 3.

Algorithm 1: Amplitude Modulation

Input: Time series $\mathbf{y} \in \mathbb{R}^T$
Output: Augmented time series \mathbf{y}_{aug}

- 1 $k \sim \text{Uniform}(0, 5)$; // Number of changepoints
- 2 Sample k changepoints $\{c_1, \dots, c_k\} \subset \{1, \dots, T - 1\}$;
- 3 $\mathbf{c} \leftarrow [0, \text{sorted}(\{c_1, \dots, c_k\}), T]$;
- 4 Sample amplitudes $\mathbf{a} \sim \mathcal{N}(1, 1)^{k+2}$;
- 5 Interpolate trend $\mathbf{t} \in \mathbb{R}^T$ from (\mathbf{c}, \mathbf{a}) ;
- 6 $\mathbf{y}_{\text{aug}} \leftarrow \mathbf{y} \odot \mathbf{t}$;
- 7 **return** \mathbf{y}_{aug}

Algorithm 2: Censor Augmentation

Input: Time series $\mathbf{y} \in \mathbb{R}^T$
Output: Augmented time series \mathbf{y}_{aug}

- 1 Sample quantile level $q \sim \text{Uniform}(0, 1)$;
- 2 Compute threshold $c \leftarrow \text{Quantile}(\mathbf{y}, q)$;
- 3 Sample censor direction $b \sim \text{Bernoulli}(0.5)$; // Bottom or top censor
- 4 **if** $b = 1$ **then**
- 5 | $\mathbf{y}_{\text{aug}} \leftarrow \max(y_t, c)$ for all t ; // Bottom censoring
- 6 **else**
- 7 | $\mathbf{y}_{\text{aug}} \leftarrow \min(y_t, c)$ for all t ; // Top censoring
- 8 **return** \mathbf{y}_{aug}

Algorithm 3: Spike Injection

Input: Time series $\mathbf{y} \in \mathbb{R}^T$ spike patterns \mathcal{P} , spike kernel set \mathcal{K} **Output:** Augmented time series \mathbf{y}_{aug}

- 1 Sample periodicity $\pi \sim \mathcal{U}(10, \min(512, T))$;
 - 2 Sample periodic pattern $z \in \mathcal{P}$ and shift it randomly ;
 - 3 Sample $s \sim \mathcal{U}(T - \pi, T)$;
 - 4 Generate spike positions $\mathbf{m} \in \mathbb{Z}^T$ by repeating z with spacing π and shifting to align last spike at s ;
 - 5 Sample kernel type $\kappa \in \mathcal{K}$;
 - 6 For each unique spike label in \mathbf{m} , sample kernel parameters and generate kernel centered at each occurrence ;
 - 7 Sum kernels to obtain additive spike signal $\mathbf{s} \in \mathbb{R}^T$;
 - 8 $\mathbf{y}_{\text{aug}} \leftarrow \mathbf{y} + \mathbf{s}$;
 - 9 **return** \mathbf{y}_{aug}
-

Table 2: Kernel types and parameterizations (as functions of the periodicity π) employed for the spike injection augmentations

Kernel	Width Param	Amplitude Param
Tophat	$w \sim [0.05\pi, 0.2\pi]$	$h \sim [0.5, 3]$
RBF	$\sigma_{\text{RBF}} \sim [0.05\pi, 0.2\pi]$	$h \sim [0.5, 3]$
Linear	$w \sim [0.05\pi, 0.2\pi]$	$h \sim [0.5, 3]$

Table 3: Spike pattern, representative patterns, and sampling probabilities employed for the spike injection augmentations.

Category	Utilized Pattern	Sample Probability
Simple	$[0], [0, 1]$	0.75
3-periodic	$[0, 1, 2], [0, 0, 1]$	0.10
4-periodic	$[0, 0, 1, 1], [0, 1, 0, 2]$	0.10
Weekly-like	$[0, 0, 0, 0, 0, 1, 1], [0, 0, 0, 0, 0, 1, 2]$	0.05

C Experiment Details

C.1 Model and Training Hyperparameter

TiRex utilizes a xLSTM-based architecture with hyperparameters summarized in Table 4. The model has 35 million model parameters.

Pre-Training TiRex is pre-trained for 500,000 steps with a batch size of 256 using the AdamW optimizer with a learning rate of 0.001 and weight decay of 0.01. We also employ a cosine learning rate scheduler with linear warm-up (the warm-up ratio is set to 5 % and the minimum learning rate is 0.0001). The context of TiRex length is 2048.

Table 4: TiRex model architecture hyperparameters.

Parameter	Value
Input patch size (m_{in})	32
Output patch size (m_{out})	32
Embedding dimension (d)	512
Feed-forward dimension (d_{ff})	2048
Number of heads	4
Number of blocks	12

C.2 Pre-Training Data Corpus

We construct a diverse training corpus by combining real and synthetic time series to support robust generalization across heterogeneous forecasting tasks. Our training dataset has three components:

- Chronos Training Data** (30 million time series): We incorporate the training datasets from Chronos and adopt their proposed time series mixup augmentation strategy (Ansari et al., 2024a). In contrast to Chronos, we generate significantly more and longer time series, expanding the diversity and temporal span of the data. Table 5 lists the respective datasets, which are provided on HuggingFace: https://HuggingFace.co/datasets/autogluon/chronos_datasets. Details on the TsMixup procedure are provided in the paragraph below.
- Synthetic Gaussian Process Data** (15 million time series): Inspired by KernelSynth (Ansari et al., 2024a), we generate synthetic time series using Gaussian Processes (GPs). Details on the synthetic data generation procedure are provided in the paragraph below.
- GiftEval Pre-training Data** (≈ 2.5 million time series): We integrate a subset of the pre-training corpus from GiftEval and use it for pre-training. It does not overlap with the GiftEval benchmark evaluation data. Table 6 lists the respective datasets, which are provided on HuggingFace: <https://HuggingFace.co/datasets/Salesforce/GiftEvalpre-train>.

Data Mix Probabilities For the Chronos training data and the synthetic Gaussian process data, each time series is sampled with equal probability. The GiftEval Pre-training data is sampled with a probability of approximately 8%, hence slightly oversampled compared to the share of series due to technical implementation details.

TsMixup To augment data diversity, we apply TsMixup (Ansari et al., 2024a), a convex combination of k time series of length l to the training data from Chronos. Each series is z -score normalized (Chronos used mean normalization) prior to combination to ensure comparable magnitude. The number k is sampled uniformly from $\{1, \dots, K_{max}\}$, the length l is sampled uniformly from $[L_{min}, L_{max}]$, and the mixing weights λ_i are drawn from a Dirichlet distribution:

$$\mathbf{x}_{1:l}^{mix} = \sum_{i=1}^k \lambda_i \cdot \tilde{\mathbf{x}}_{1:l}^i, \tag{10}$$

where $\tilde{\mathbf{x}}_i \in \mathbb{R}^l$ is a normalized time series segment, and $\boldsymbol{\lambda} \sim \text{Dir}(\alpha)$. As $k = 1$ is sampled with non-zero probability, the augmented dataset includes original sequences, thereby preserving base

data fidelity while enhancing variability. In our procedure we utilize $K_{\max} = 4$, $L_{\min} = 128$, $L_{\min} = 4096$, and $\alpha = 1.5$; we generate 30 million time series.

Synthetic GP Data We generate synthetic time series using Gaussian Processes (GPs), building upon the core ideas of KernelSynth (Ansari et al., 2024a). Each synthetic time series $\mathbf{x} \in \mathbb{R}^{L_{\text{syn}}}$ is sampled from a GP:

$$\mathbf{x} \sim \mathcal{GP}(0, \tilde{\kappa}(t, t')), \quad (11)$$

where $\tilde{\kappa}(t, t')$ is a composite kernel constructed by randomly sampling and combining kernels from a kernel bank \mathcal{K} . We sample $j \sim U\{1, J\}$ base kernels (with replacement) from \mathcal{K} and combine them using random binary operations from $\{+, \times\}$ to obtain $\tilde{\kappa}$. Kernel parameters (e.g., length scale, periodicity) are sampled from predefined priors. In our procedure, we utilize $J = 4$ and $L_{\text{syn}} = 4096$; Our kernel bank \mathcal{K} includes periodic, Radial Basis Function (RBF), Rational Quadratic (RQ), and Piecewise Polynomial kernels. We generate 15 million time series with this procedure.

In contrast to KernelSynth, we introduce the following adaptations:

1. We sample periodicities from both fixed sets (as KernelSynth) and additionally from continuous distributions to increase temporal diversity.
2. We employ a more scalable GP sampler with GPU support and approximations for longer series (Gardner et al., 2018). This enables the generation of more and longer sequences.
3. We use a modified kernel bank.

Table 5: Training Datasets published by Ansari et al. (2024a) — (https://huggingface.co/datasets/autogluon/chronos_datasets) — that were utilized to train TiRex.

Name	#Series	Avg. Length
Mexico City Bikes	494	78313
Brazilian Cities Temperature	12	757
Solar (5 Min.)	5166	105120
Solar (Hourly)	5166	105120
Spanish Energy and Weather	66	35064
Taxi (Hourly)	2428	739
USHCN	6090	38653
Weatherbench (Hourly)	225280	350639
Weatherbench (Daily)	225280	14609
Weatherbench (Weekly)	225280	2087
Wiki Daily (100k)	100000	2741
Wind Farms (Hourly)	100000	8514
Wind Farms (Daily)	100000	354
Electricity (15 Min.)	370	113341
Electricity (Hourly)	321	26304
Electricity (Weekly)	321	156
KDD Cup 2018	270	10897
London Smart Meters	5560	29951
M4 (Daily)	4227	2371
M4 (Hourly)	414	901
M4 (Monthly)	48000	234
M4 (Weekly)	359	1035
Pedestrian Counts	66	47459
Rideshare	2340	541
Taxi (30 Min.)	2428	1478
Temperature-Rain	32072	725
Uber TLC (Hourly)	262	4344
Uber TLC (Daily)	262	181

Table 6: Subset of pre-training datasets published by Aksu et al. (2024) — (<https://huggingface.co/datasets/Salesforce/GiftEvalPretrain>) — that were utilized to train TiRex.

Name	#Series	Avg. Length
azure vm traces 2017	159472	5553
borg cluster data 2011	143386	3749
bdg-2 panther	105	8760
bdg-2 fox	135	17219
bdg-2 rat	280	16887
bdg-2 bear	91	16289
lcl	713	13385
smart	5	19142
ideal	217	5785
sceaux	1	34223
borealis	15	5551
buildings 900k	1795256	8761
largest 2017	8196	105120
largest 2018	8428	105120
largest 2019	8600	105120
largest 2020	8561	105408
largest 2021	8548	105120
PEMS03	358	26208
PEMS04	307	16992
PEMS07	883	28224
PEMS08	170	17856
PEMS BAY	325	52128
LOS LOOP	207	34272
BEIJING SUBWAY 30MIN	276	1572
SHMETRO	288	8809
HZMETRO	80	2377
Q-TRAFFIC	45148	5856
subseasonal	862	16470
subseasonal precip	862	11323
wind power	1	7397147
solar power	1	7397222
kaggle web traffic weekly	145063	114
kdd2022	134	35280
godaddy	3135	41
favorita sales	111840	1244
china air quality	437	13133
beijing air quality	12	35064
residential load power	271	538725
residential pv power	233	537935
cdc fluvview ilinet	75	852
cdc fluvview who	74	564

C.3 Benchmarks and Metrics

We evaluated our models on two standardized benchmarks, GiftEval (Aksu et al., 2024) and the Chronos Zero-Shot benchmark (Ansari et al., 2024a). Both are hosted on public HuggingFace leaderboards. These benchmarks offer transparent, reproducible evaluations across a wide range of datasets, domains, and forecast horizons, enabling a comprehensive assessment of generalization capabilities. The benchmarks not only specify the datasets and forecast horizons but also metric computations, and provide results of state-of-the-art models, ensuring valid baseline comparisons.

GiftEval. GiftEval (Aksu et al., 2024) comprises 23 datasets totaling over 144,000 time series, spanning seven domains, ten sampling frequencies, and a wide range of forecast horizons from short- to long-term. In sum the benchmark evaluates 97 different evaluation settings. The benchmark includes evaluations of 17 models, covering classical statistical methods, deep learning approaches, and recent foundation models, including all pre-trained models relevant to our study.

In total, 16 out of the 97 evaluation settings in GiftEval overlap with those used for pre-training in our work (i.e., the Chronos pre-train collection). To ensure comparability while avoiding data leakage, we restrict our main evaluation to non-overlapping datasets. We denote this benchmark as **GiftEval-ZS benchmark**. This is possible because of the dataset-level granularity of the leaderboard submissions, which allows custom aggregations of results while preserving fidelity to the original benchmark. Full benchmark results, including the overlapping datasets, are reported in Appendix D.1. The individual datasets and evaluation settings of the benchmark are listed in Table 8. For additional details, please refer to Aksu et al. (2024).

GiftEval uses the Mean Absolute Scaled Error (MASE) for point forecasts and the Continuous Ranked Probability Score (CRPS) for probabilistic forecasts as performance metrics. Equation 12 defines the MASE: \hat{y}_t is the point forecast, y_t is the observed value at time t . MASE scales the error by a naïve seasonal forecast, given the seasonal period s . Equation 13 respectively defines the CRPS: $F(u)$ is the predictive cumulative distribution and $\mathbf{1}\{y_t \leq u\}$ is the indicator function for the observed value. To evaluate performance over a full forecast horizon, the CRPS is averaged across time steps. In practice, CRPS is approximated by computing the average weighted quantiles loss over a fixed set of quantile levels $Q = \{0.1, 0.2, \dots, 0.9\}$, with \hat{y}_t^q as the quantile prediction of quantile q at time step t (see Equation 14).

$$\text{MASE} = \frac{\frac{1}{h} \sum_{t=T+1}^{T+h} |\hat{y}_t - y_t|}{\frac{1}{h} \sum_{t=s+1}^T |y_t - y_{t-s}|} \quad (12)$$

$$\text{CRPS} = \frac{1}{h} \sum_{t=T+1}^{T+h} \int_{-\infty}^{\infty} (F(u) - \mathbf{1}\{y_t \leq u\})^2 du \quad (13)$$

$$\text{CRPS} \approx \frac{1}{|Q| \cdot h} \sum_{q \in Q} \frac{2 \sum_{t=T+1}^{T+h} \text{QL}(q, \hat{y}_t^q, y_t)}{\sum_{t=T+1}^{T+h} |y_t|} \quad (14)$$

$$\text{QL}(q, \hat{y}_t^q, y_t) = \begin{cases} q(y_t - \hat{y}_t^q) & \text{if } \hat{y}_t^q \leq y_t \\ (1-q)(\hat{y}_t^q - y_t) & \text{else.} \end{cases} \quad (15)$$

Before aggregation, the metric values of both metrics are normalized per dataset using a seasonal naïve baseline to mitigate scale effects. The aggregated metric scores are computed using the geometric mean of these normalized scores. Additionally, the average rank of the CRPS across evaluation settings is reported to increase robustness against outlier results.

Chronos-ZS benchmark. The Chronos-ZS benchmark (Ansari et al., 2024a) consists of 27 datasets, with a focus on short-term forecasting. TiRex’s pre-training data has no overlap with Chronos-ZS benchmark, hence we can use it to extend the assessment of its zero-shot capabilities. The evaluation metrics are identical in structure to GiftEval: MASE for point forecasts and Weighted Quantile Loss (WQL) for probabilistic forecasts, with WQL evaluated over the same set of quantiles, making it computationally equivalent to the CRPS approximation of GiftEval. Aggregation procedures,

including baseline normalization and geometric mean computation, are also consistent across both benchmarks. The datasets and settings of the benchmark are presented in Table 8; for additional details, please refer to Ansari et al. (2024a).

C.4 Computation & Hardware

We conducted all experiments on Nvidia A40 and H100 GPUs — A40's provide enough GPU memory to conduct all training runs. The inference experiments (GPU memory and Inference Speed) were conducted on a Nvidia A40 GPU. CPU requirements are flexible; we utilized a 64-core Xeon(R) Platinum 8358.

Table 7: GiftEval (Aksu et al., 2024) benchmark datasets and evaluation settings. Evaluation settings that are part of GiftEval-ZS benchmark are marked in the respective column. Forecast Horizon is abbreviated as “Hor” and the number of evaluated windows is abbreviated as “Win”.

Name	GiftEval-ZS	Freq	#Series	Short		Medium		Long	
				Hor	Win	Hor	Win	Hor	Win
bitbrains_fast_storage	x	5T	1250	48	18	480	2	720	2
bitbrains_fast_storage	x	H	1250	48	2	-	-	-	-
bitbrains_rnd	x	5T	500	48	18	480	2	720	2
bitbrains_rnd	x	H	500	48	2	-	-	-	-
bizitobs_application	x	10S	1	60	15	600	2	900	1
bizitobs_l2c	x	5T	1	48	20	480	7	720	5
bizitobs_l2c	x	H	1	48	6	480	1	720	1
bizitobs_service	x	10S	21	60	15	600	2	900	1
car_parts	x	M	2674	12	1	-	-	-	-
covid_deaths	x	D	266	30	1	-	-	-	-
electricity		15T	370	48	20	480	20	720	20
electricity	x	D	370	30	5	-	-	-	-
electricity		H	370	48	20	480	8	720	5
electricity		W	370	8	3	-	-	-	-
ett1	x	15T	1	48	20	480	15	720	10
ett1	x	D	1	30	3	-	-	-	-
ett1	x	H	1	48	20	480	4	720	3
ett1	x	W	1	8	2	-	-	-	-
ett2	x	15T	1	48	20	480	15	720	10
ett2	x	D	1	30	3	-	-	-	-
ett2	x	H	1	48	20	480	4	720	3
ett2	x	W	1	8	2	-	-	-	-
hierarchical_sales	x	D	206	30	4	-	-	-	-
hierarchical_sales	x	W	118	8	4	-	-	-	-
hospital	x	M	767	12	1	-	-	-	-
jena_weather	x	10T	1	48	20	480	11	720	8
jena_weather	x	D	1	30	2	-	-	-	-
jena_weather	x	H	1	48	19	480	2	720	2
kdd_cup_2018		D	270	30	2	-	-	-	-
kdd_cup_2018		H	270	48	20	480	2	720	2
loop_seattle	x	5T	323	48	20	480	20	720	15
loop_seattle	x	D	323	30	2	-	-	-	-
loop_seattle	x	H	323	48	19	480	2	720	2
m4_daily		D	4227	14	1	-	-	-	-
m4_hourly		H	207	48	2	-	-	-	-
m4_monthly		M	2400	18	20	-	-	-	-
m4_quarterly	x	Q	24000	8	1	-	-	-	-
m4_weekly		W	359	13	1	-	-	-	-
m4_yearly	x	A	22974	6	1	-	-	-	-
m_dense	x	D	30	30	3	-	-	-	-
m_dense	x	H	30	48	20	480	4	720	3
restaurant	x	D	403	30	2	-	-	-	-
saugeen	x	D	1	30	20	-	-	-	-
saugeen	x	M	1	12	7	-	-	-	-
saugeen	x	W	1	8	20	-	-	-	-
solar	x	10T	137	48	20	480	11	720	8
solar	x	D	137	30	2	-	-	-	-
solar	x	H	137	48	19	480	2	720	2
solar	x	W	137	8	1	-	-	-	-
sz_taxi	x	15T	156	48	7	480	1	720	1
sz_taxi	x	H	156	48	2	-	-	-	-
temperature_rain		D	32072	30	3	-	-	-	-
us_births	x	D	1	30	20	-	-	-	-
us_births	x	M	1	12	2	-	-	-	-
us_births	x	W	1	8	14	-	-	-	-

Table 8: Chronos-ZS benchmark benchmark datasets (Ansari et al., 2024a) and evaluation setting.

Name	Horizon	Periodicty
traffic	24	24
australian electricity	48	48
ercot	24	24
ETTm	24	96
ETTth	24	24
exchange rate	30	5
nn5	56	1
nn5 weekly	8	1
weather	30	1
covid deaths	30	1
fred md	12	12
m4 quarterly	8	4
m4 yearly	6	1
dominick	8	1
m5	28	1
tourism monthly	24	12
tourism quarterly	8	4
tourism yearly	4	1
car parts	12	12
hospital	12	12
cif 2016	12	12
m1 yearly	6	1
m1 quarterly	8	4
m1 monthly	18	12
m3 monthly	18	12
m3 yearly	6	1
m3 quarterly	8	4

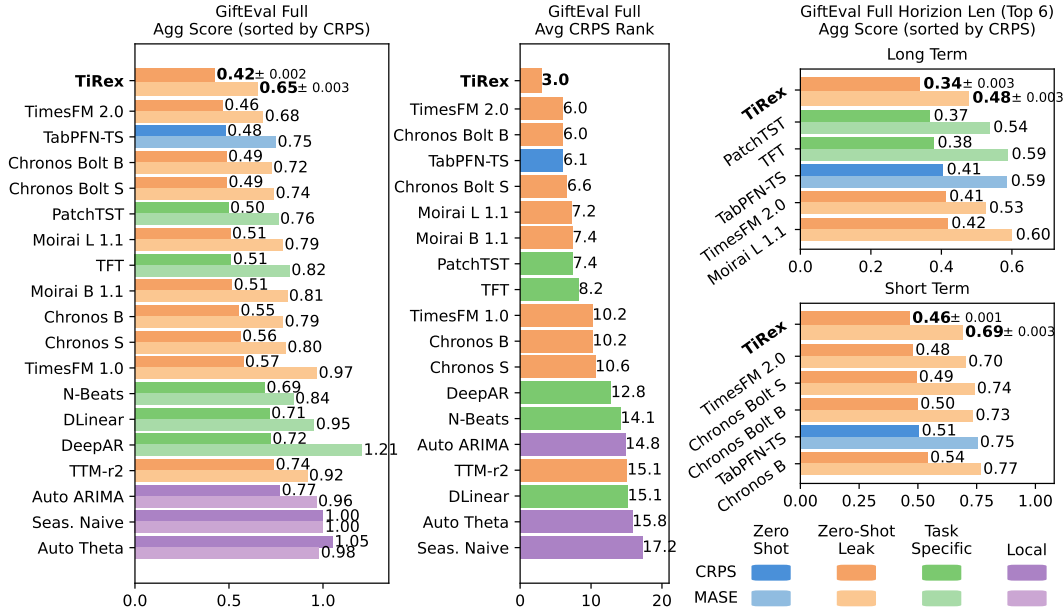


Figure 8: Results of the full GiftEval benchmark: Aggregated scores of the overall benchmark and the short- and long-term performances. Additionally, the average rank in terms of CRPS, as in the public leaderboard, is presented. Lower values are better. “Zero-shot Leak” refers to models which are partly trained on the benchmark datasets. We trained TiRex with 6 different seeds and report the observed standard deviation in the plot.

D Extended Results

This section presents additional experimental results complementing Section 4. The structure is the same as in the main paper, preceded by results for the full GiftEval benchmark: First, extended results on the zero-shot evaluation of GiftEval-ZS benchmark and Chronos-ZS benchmark are presented, followed by inference efficiency results of all pre-trained models, extended ablation studies results, and additional qualitative examples. Additionally, we provide fine-tuning results.

D.1 Full GiftEval leaderboard

Figure 8 presents the evaluation results on the full GiftEval benchmark, including settings excluded from GiftEval-ZS benchmark due to training data overlap with TiRex. These results align with those reported on the HuggingFace GiftEval leaderboard. The results are consistent with the trends observed in the main GiftEval-ZS benchmark evaluation. TiRex outperforms all baseline models by a substantial margin, with the largest performance gap observed in the long-term forecasting tasks.

D.2 Zero-Shot Forecasting

GiftEval-ZS benchmark Figures 9–11 present the short-, medium-, and long-term evaluation sub-results for all models. Both aggregated scores and average CRPS rank metrics are reported. As discussed in the main text, TiRex consistently achieves the best performance across all settings. The results of the individual evaluation settings are reported in the Tables 9-16.

Chronos-ZS benchmark Figure 12 extends the Chronos benchmark results by including task-specific and local models not covered by the official leaderboard, which reports only pre-trained models. These additional results are taken from the benchmark’s original publication (Ansari et al., 2024a). Consistent with the main paper, TiRex performs best and even outperforms models with substantial training data overlap and those explicitly trained for individual datasets. The results of the individual evaluation settings are reported in the Tables 17-18.

Inference Efficiency Figure 13 presents an extended inference efficiency comparison, including additional pre-trained baselines beyond those shown in the main paper.

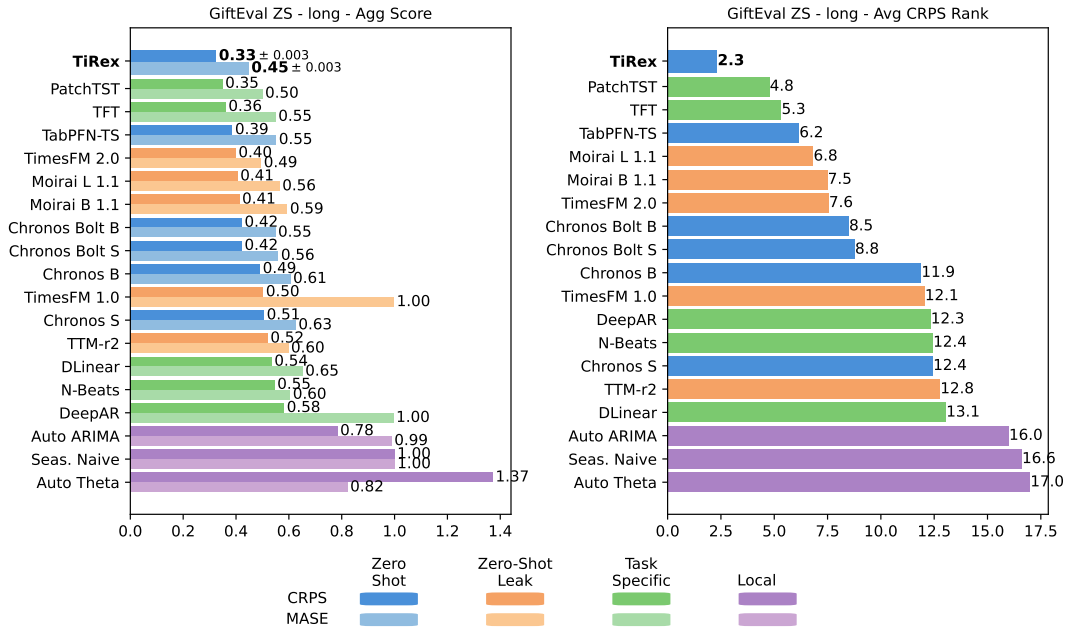


Figure 9: Results of the GiftEval-ZS benchmark: The aggregated scores and the average CRPS rank of the benchmarks’ **long-term** sub-results are shown. Lower values are better. “Zero-shot Leak” refers to models that are partly trained on the benchmark datasets. We trained TiRex with 6 different seeds and report the observed standard deviation of the aggregated scores.

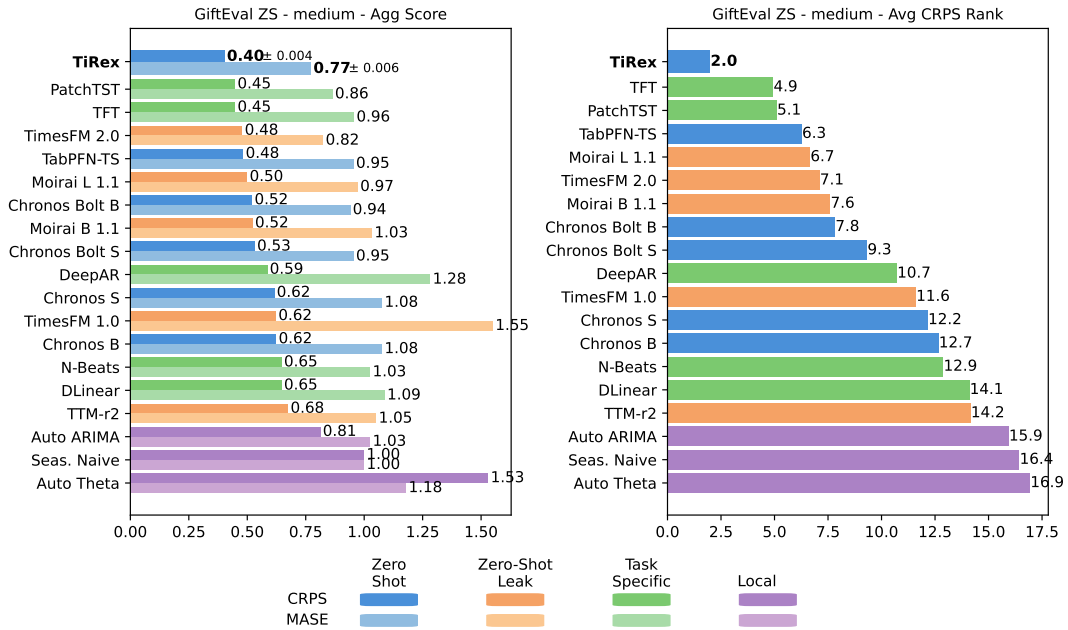


Figure 10: Results of the GiftEval-ZS benchmark: The aggregated scores and the average CRPS rank of the benchmarks' **medium-term** sub-results are shown. Lower values are better. "Zero-shot Leak" refers to models that are partly trained on the benchmark datasets. We trained TiRex with 6 different seeds and report the observed standard deviation of the aggregated scores.

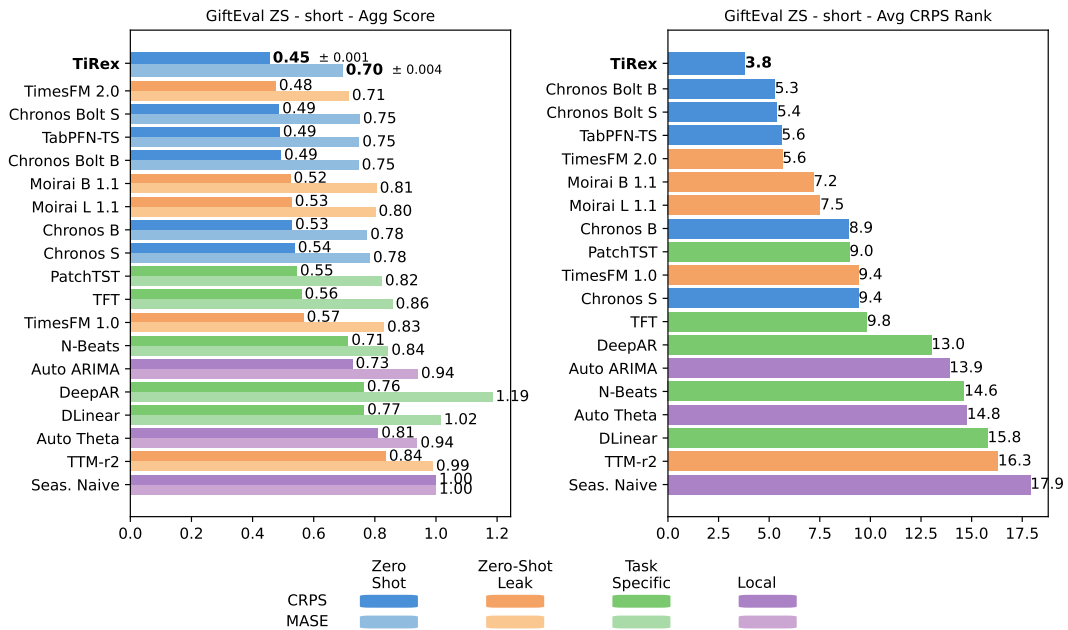


Figure 11: Results of the GiftEval-ZS benchmark: The aggregated scores and the average CRPS rank of the benchmarks' **short-term** sub-results are shown. Lower values are better. "Zero-shot Leak" refers to models that are partly trained on the benchmark datasets. We trained TiRex with 6 different seeds and report the observed standard deviation of the aggregated scores.

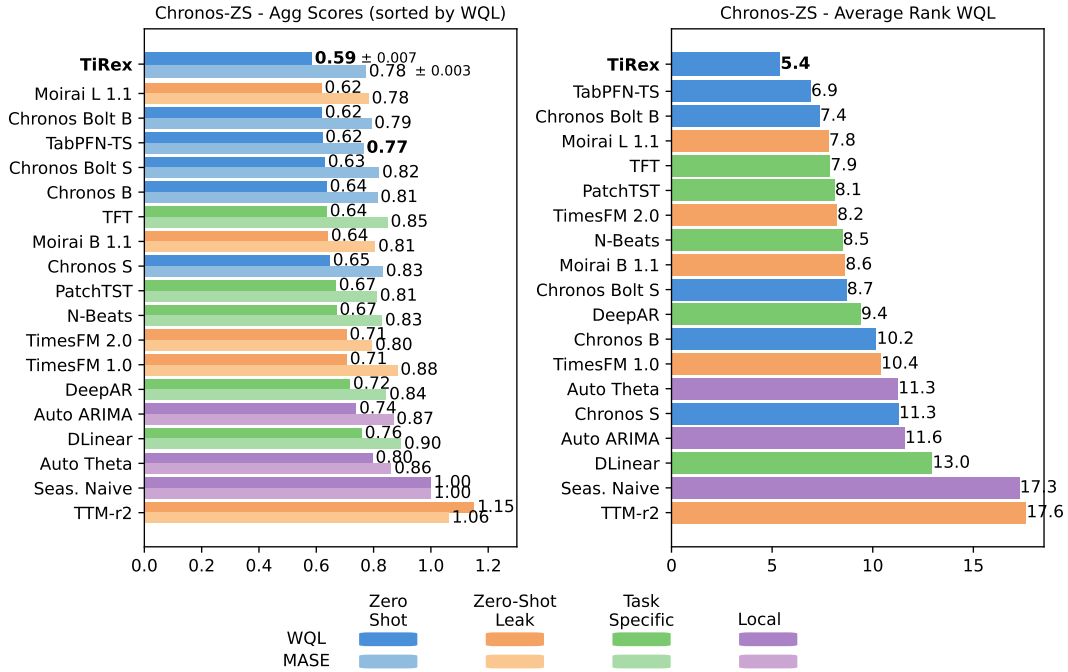


Figure 12: Results of the Chronos-ZS benchmark: The aggregated scores and the average WQL rank. Lower values are better. “Zero-shot Leak” refers to models that are partly trained on the benchmark datasets (Overlap: Moirai 82%, TimesFM 15%, TTM: 11%). We trained TiRex with 6 different seeds and report the observed standard deviation of the aggregated scores.

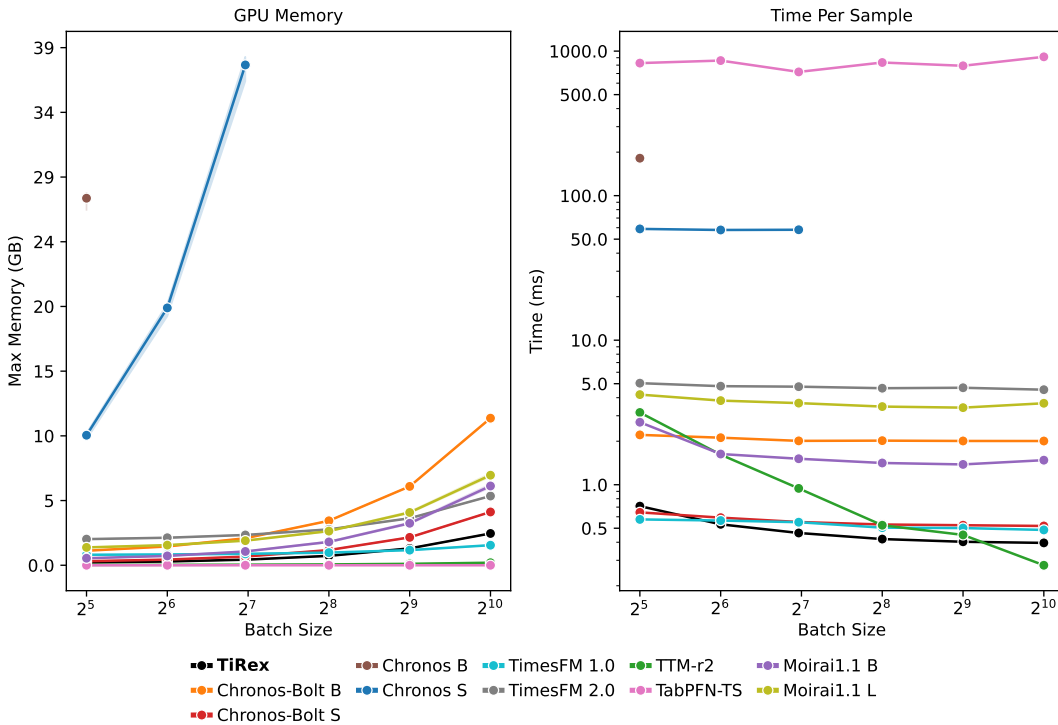


Figure 13: Inference efficiency of different pre-trained forecasting models. Left: GPU Memory depending on the batch size. The maximum available GPU memory was 48 GB in the experiment (Nvidia A40). Right: Inference Time per sample depending on the batch size.

D.3 Ablations

Contiguous Patch Masking (CPM) CPM applies 2 hyperparameters: $p_{\text{mask}}^{\text{max}}$, which defines the maximum masking probability sampled per sample, and $c_{\text{mask}}^{\text{max}}$, which defines the maximum for the number of consecutive patches sampled per sample. As pre-training computational demand hinders an extended hyperparameter search, we heuristically selected $p_{\text{mask}}^{\text{max}} = 0.25$, which corresponds to a typical dropout probability of time series models, and $c_{\text{mask}}^{\text{max}} = 5$ to ensure multi-patch forecasts spanning multiple tokens. To analyze the sensitivity of the model performance to these parameters, we additionally trained TiRex variants spanning the combinations of $p_{\text{mask}}^{\text{max}} = \{0.1, 0.25, 0.5\}$ and $c_{\text{mask}}^{\text{max}} = \{0, 1, 3, 5, 7, 9\}$. Figure 14 illustrates the results: The results are not very sensitive to the parameters as long as CPM is utilized ($c_{\text{mask}}^{\text{max}} > 0$). Additionally, good long-term forecasts require sufficient training samples with multi-patch forecasts spanning multiple tokens, i.e., $c_{\text{mask}}^{\text{max}} > 3$ or $p_{\text{mask}}^{\text{max}} \geq 0.5$ (the latter more likely leads to neighboring masked patches that effectively mask out more than $c_{\text{mask}}^{\text{max}}$ patches).

Augmentations We do not apply each augmentation to every sample. Due to the computational cost of pre-training, an extensive hyperparameter search was not feasible. Instead, we heuristically selected application probabilities under the hypothesis that augmentations are beneficial, but excessive use may lead to diminished returns. We chose an application probability of 0.5 for both Censor and Amplitude Modulation. For Spike Injection, we used a lower probability of 0.05, as its computational cost is higher, and frequent application creates a speed bottleneck in training.

To analyze the sensitivity of TiRex’s performance to these application probabilities, we trained additional variants with altered values. Specifically, we tested probabilities in $\{0, 0.1, 0.25, 0.75, 1\}$ for Censor and Amplitude Modulation, and probabilities in $\{0, 0.01, 0.2, 0.3\}$ for Spike Injection. Figure 15 summarizes the results. The analysis indicates that model performance is relatively robust to variations in application probability as long as the augmentations are utilized at all. However, targeted tuning may yield marginal improvements.

Chronos-Bolt architecture trained with our data pipeline In order to isolate the impact of our dataset and augmentation pipeline from other methodological contributions, we trained a Chronos-Bolt architecture, as representative of a state-of-the-art pre-trained model. Chronos-Bolt was selected due to its publicly available code and configuration, though the exact training data and procedure remain undisclosed. We used the same training hyperparameters (e.g., learning rate, warmup schedule, . . .) as for TiRex. Figure 16 shows that integrating our data pipeline leads to improved performance compared to the published Chronos-Bolt results on the GiftEval-ZS benchmark, while we see a mixed effect on the Chronos-ZS benchmark. Nonetheless, TiRex consistently outperforms the optimized Chronos-Bolt variant, which highlights the contributions of both CPM and the xLSTM backbone to TiRex’s effectiveness. This difference is most pronounced for long-term forecasts.

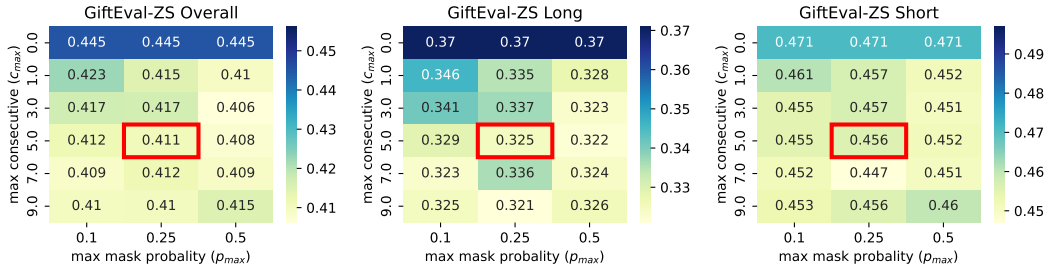


Figure 14: CRPS results on the GiftEval-ZS benchmark of TiRex variants trained with a different set of hyperparameters for Contiguous Patch Masking ($c_{\text{mask}}^{\text{max}} = 0$ indicates that Contiguous Patch Masking is not used). The parameters used for training TiRex are enclosed in a red frame.

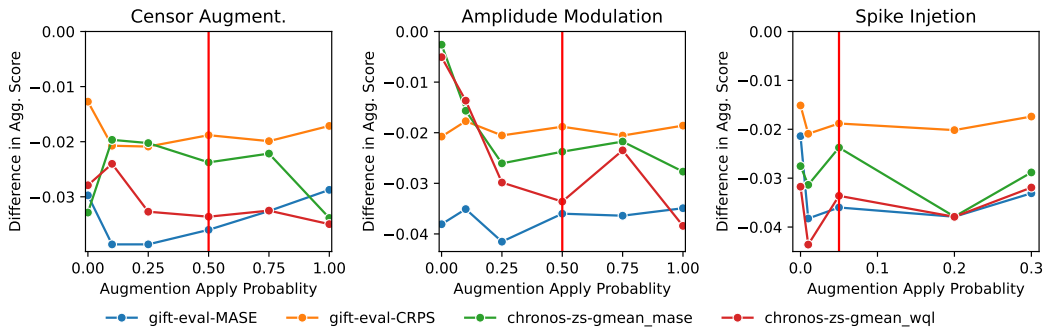


Figure 15: CRPS performance variation on the GiftEval-ZS benchmark for TiRex variants trained with different augmentation application probabilities, relative to a baseline TiRex without augmentations. Red vertical lines indicate the parameters used in the actual model configuration.

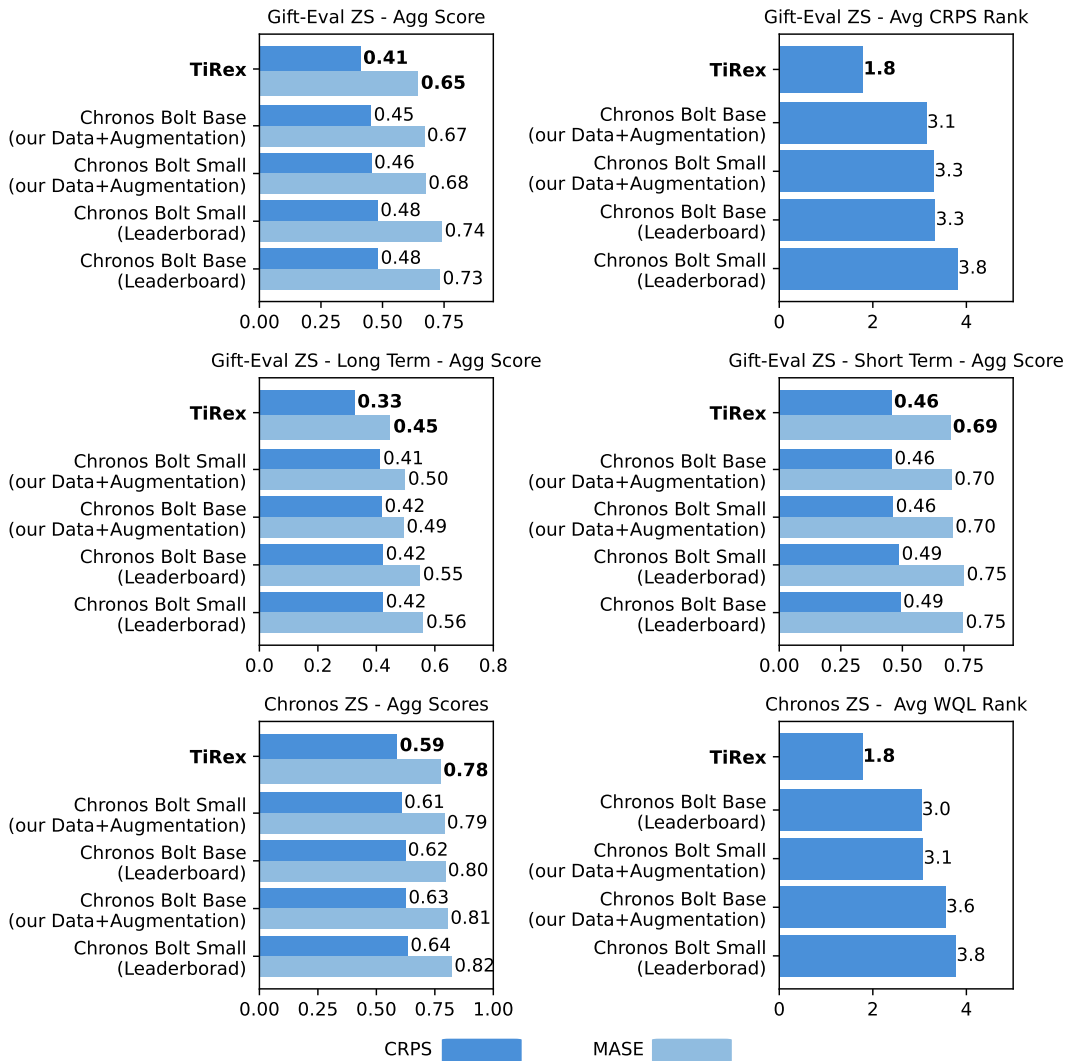


Figure 16: Results of training a Chronos-Bolt architecture with the same data and data augmentations as TiRex — compared to the published Chronos-Bolt model and TiRex. The results are from the GiftEval-ZS benchmark and the Chronos-ZS benchmark.

D.4 Additional qualitative examples

In addition to Figure 1 from the main paper, we provide further qualitative examples of forecasts on the GiftEval benchmark. Specifically, Figure 18 depicts the model behaviors for medium- and long-term forecasts and Figure 19 does the same for short-term forecasts.

D.5 Finetuned-Forecasting

To further explore the capabilities of our already strong pre-trained model, we finetune TiRex with the training split of the GiftEval benchmark (as defined by Aksu et al., 2024). Fine-tuning is performed jointly across all training datasets. To avoid overfitting, we mix the training data with our pre-training data, using a 20/80 ratio. For sampling, we use a uniform distribution to choose the dataset to draw the next training sample from. We freeze the input and output layers of TiRex and run over 40k steps with an initial learning rate of 1×10^{-3} and a linear learning rate decay that reaches 0 at the end of the run. In contrast to the pre-training regime, we do not apply any data augmentation techniques (see Section 3) but still employ CPM (Section 2.1).

In the finetuning setting, we observe an incremental improvement over the pre-trained model, especially in the MASE metric (Figure 17). Specifically, we compare the pre-trained to its finetuned version as well as to a fine-tuned TTM (Ekambaram et al., 2024), the only zero-shot model that provides fine-tune results on the GiftEval leaderboard.

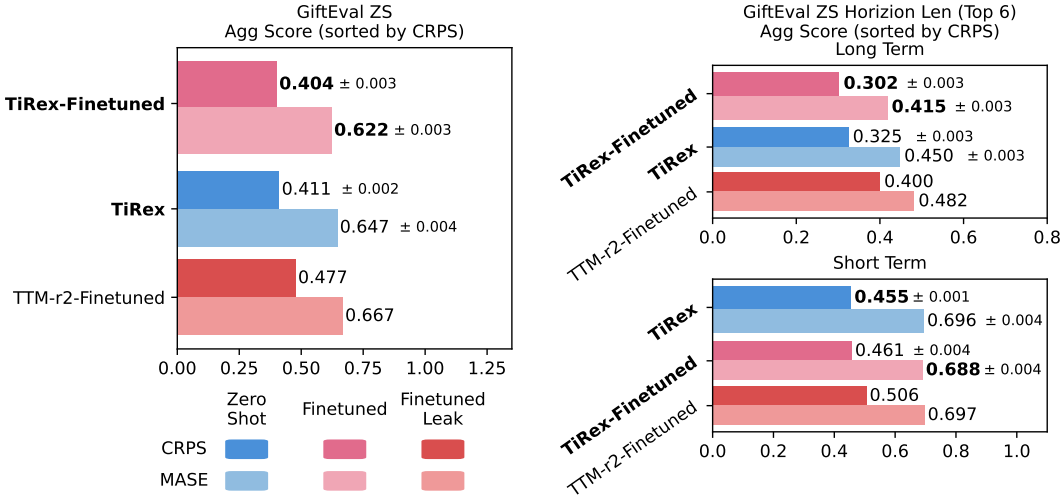


Figure 17: GiftEval-ZS benchmark evaluation results comparing the finetuned models from the GiftEval leaderboard to our pre-trained and finetuned models. We trained TiRex with 6 different seeds, finetuned each of these models with 4 different seeds (24 seeds in total), and report the mean and the observed standard deviation of the aggregated scores.

E Societal Impact

As a pre-trained zero-shot model, TiRex could democratize access to modern forecasting techniques by removing the need for task-specific training or machine learning expertise, enabling broader adoption across non-expert communities. It also has the potential to enhance forecasting in data-sparse domains. Nonetheless, care must be taken to ensure responsible deployment, particularly in high-stakes settings where model errors could have significant real-world consequences.

F Code

The code repository for the model is hosted on GitHub: <https://github.com/NX-AI/tirex>

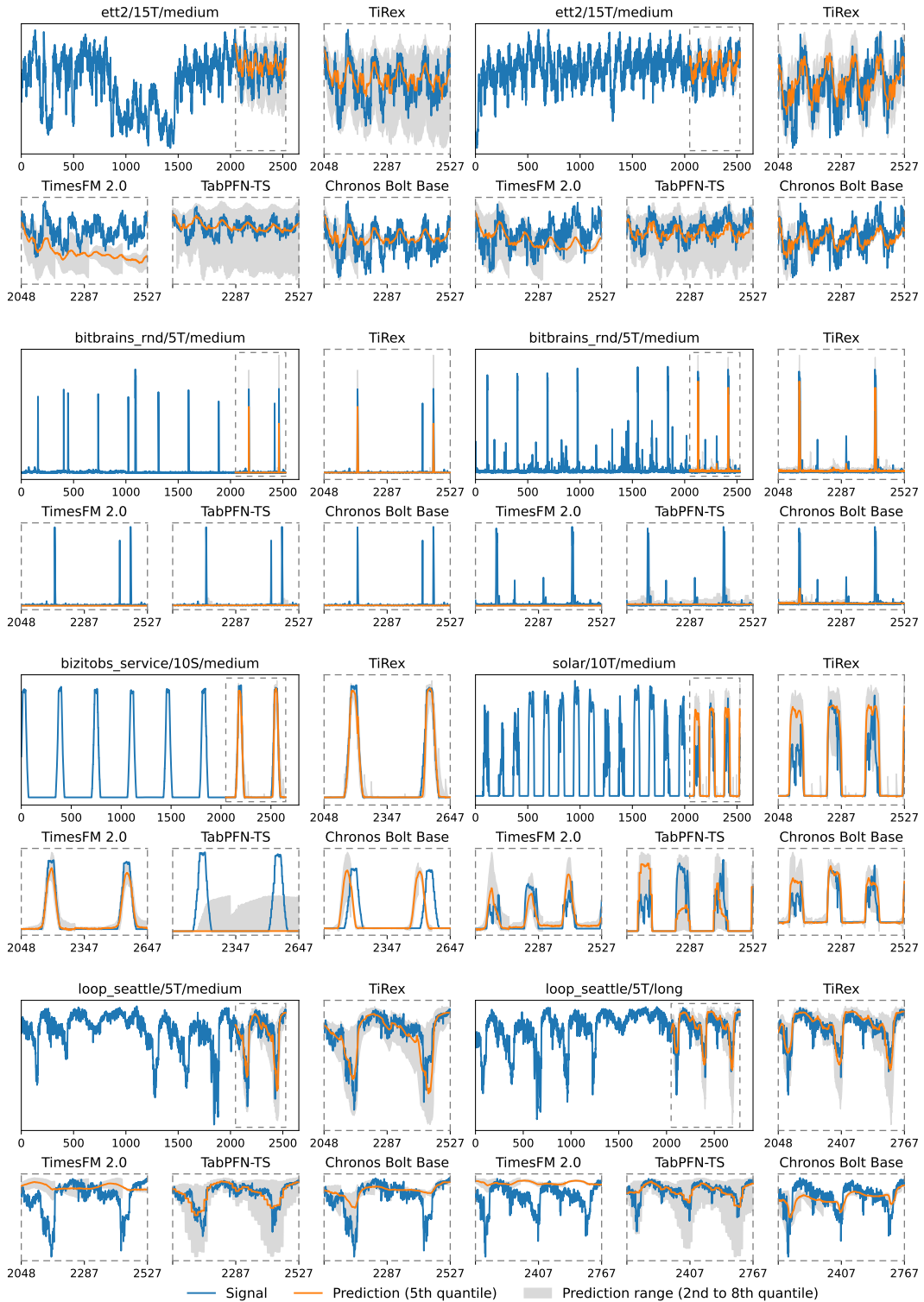


Figure 18: Examples of **medium- and long-term forecasts** from the GiftEval benchmark. For each example, we show one plot with the full context and the TiRex prediction, as well as zoomed-in forecasts of the best-performing zero-shot models.

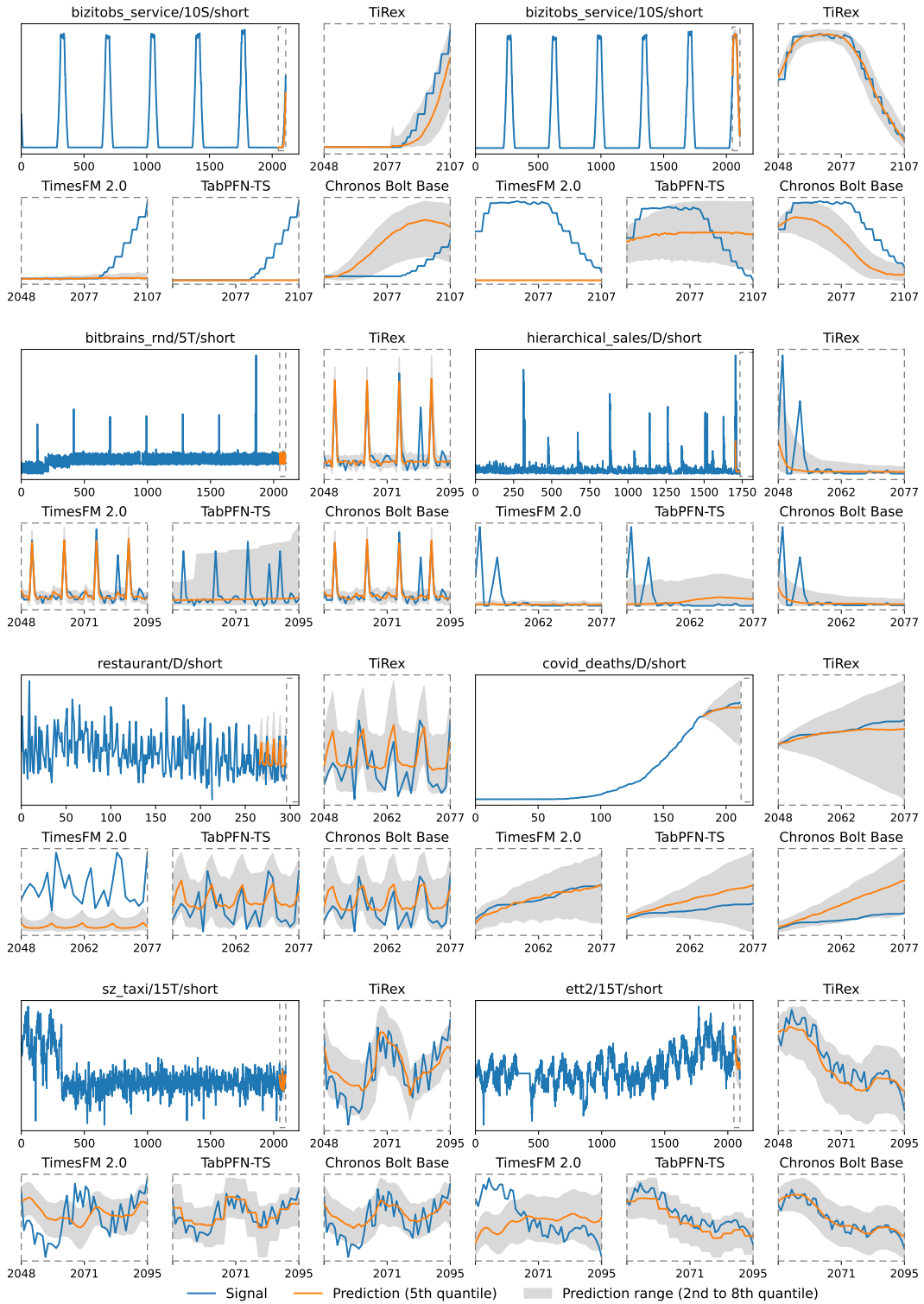


Figure 19: Examples of **short-term forecasts** from the GiftEval benchmark. For each example, we show one plot with the full context and the TiRex prediction, as well as zoomed-in forecasts of the best-performing zero-shot models.

Table 9: MASE scores of different zero-shot models on the GiftEval benchmark evaluation settings (Part 1/2). The models achieving the **best** and second-best scores are highlighted. Results for datasets that are part of the training data for the respective models are shaded in grey, and these results are excluded from the calculation of the best score. We trained TiRex with 6 different seeds and report the observed standard deviation in the plot.

	TiRex	Chronos Bolt B	Chronos Bolt S	TimesFM 2.0	TimesFM 1.0	TabPFN-TS	Moirai L 1.1	Moirai B 1.1	TTM-r2	Chronos B	Chronos S
bitbrains_fast_storage/5T/long	0.916 ± 0.006	0.948	0.962	0.980	32.0	1.04	0.955	0.967	1.16	1.01	1.08
bitbrains_fast_storage/5T/medium	1.00 ± 0.011	1.06	1.06	1.08	20.3	1.19	<u>1.02</u>	1.05	1.23	1.11	1.14
bitbrains_fast_storage/5T/short	0.692 ± 0.007	0.752	0.778	<u>0.731</u>	0.874	0.888	0.827	0.792	0.966	0.850	0.833
bitbrains_fast_storage/H/short	1.06 ± 0.013	<u>1.07</u>	1.08	1.09	1.18	1.15	1.09	1.18	1.28	1.11	1.14
bitbrains_rnd/5T/long	3.35 ± 0.013	<u>3.40</u>	3.41	3.60	91.0	3.51	3.42	3.45	3.78	3.77	3.83
bitbrains_rnd/5T/medium	4.40 ± 0.007	<u>4.45</u>	4.47	4.59	49.8	4.59	4.46	4.53	4.81	4.60	4.63
bitbrains_rnd/5T/short	1.66 ± 0.004	<u>1.71</u>	1.72	1.77	1.98	1.87	1.75	1.82	2.05	1.79	1.81
bitbrains_rnd/H/short	5.84 ± 0.011	5.90	5.88	5.99	6.09	5.96	5.93	6.07	6.16	5.79	5.89
bizitobs_application/10S/long	3.67 ± 0.069	10.5	9.65	<u>4.07</u>	16.3	7.73	7.84	13.5	9.59	9.25	9.67
bizitobs_application/10S/medium	2.85 ± 0.057	9.72	9.15	<u>3.08</u>	11.2	6.93	7.39	12.8	9.02	9.87	10.2
bizitobs_application/10S/short	1.40 ± 0.112	5.53	5.41	<u>1.56</u>	4.36	3.19	4.51	5.32	4.21	3.01	3.34
bizitobs_l2c/5T/long	<u>1.19</u> ± 0.040	1.24	1.36	<u>1.24</u>	1.28	1.22	1.12	1.12	1.32	1.20	1.25
bizitobs_l2c/5T/medium	0.849 ± 0.028	0.878	0.920	1.02	0.887	0.870	0.987	<u>0.853</u>	0.992	0.942	0.880
bizitobs_l2c/5T/short	0.290 ± 0.005	<u>0.278</u>	0.272	<u>0.312</u>	0.310	0.338	0.285	<u>0.291</u>	0.324	0.301	0.301
bizitobs_l2c/H/long	<u>0.590</u> ± 0.022	0.556	0.612	1.30	1.27	0.919	1.27	1.09	1.24	1.25	1.31
bizitobs_l2c/H/medium	<u>0.525</u> ± 0.020	0.495	0.570	1.18	1.49	0.748	1.25	1.32	1.24	1.34	1.32
bizitobs_l2c/H/short	0.528 ± 0.021	0.432	<u>0.485</u>	<u>0.782</u>	1.05	0.634	1.15	0.999	0.983	0.990	0.905
bizitobs_service/10S/long	1.57 ± 0.057	5.30	4.85	<u>2.15</u>	7.77	3.90	4.33	6.08	5.34	4.22	3.89
bizitobs_service/10S/medium	1.32 ± 0.058	4.98	4.64	<u>1.53</u>	6.46	3.78	3.87	5.99	5.12	4.58	4.06
bizitobs_service/10S/short	0.884 ± 0.052	3.32	2.90	<u>1.04</u>	2.90	2.00	2.31	3.43	2.73	1.88	1.91
car_parts/M/short	0.838 ± 0.004	0.855	0.858	0.922	0.893	<u>0.843</u>	<u>0.903</u>	<u>0.835</u>	1.57	0.908	0.885
covid_deaths/D/short	39.5 ± 0.803	38.9	36.5	47.4	55.6	<u>37.8</u>	36.5	34.6	53.5	42.7	42.2
electricity/15T/long	0.891 ± 0.008	0.933	<u>0.953</u>	0.904	1.50	<u>1.02</u>	1.31	1.32	1.35	1.01	1.06
electricity/15T/medium	0.841 ± 0.006	0.862	0.896	0.845	1.49	<u>0.977</u>	1.29	1.33	1.32	0.990	1.03
electricity/15T/short	0.945 ± 0.008	0.935	0.936	0.907	1.48	<u>1.23</u>	1.71	1.54	1.43	1.05	1.13
electricity/D/short	1.43 ± 0.010	<u>1.45</u>	1.48	1.49	1.75	1.49	1.51	1.50	1.66	1.56	1.60
electricity/H/long	<u>1.21</u> ± 0.018	1.24	1.26	1.05	<u>1.21</u>	1.34	1.36	1.26	1.38	1.20	1.23
electricity/H/medium	1.08 ± 0.010	1.08	1.10	0.929	<u>1.07</u>	1.18	1.20	1.19	1.25	1.06	1.09
electricity/H/short	0.869 ± 0.009	0.873	0.914	0.763	<u>0.878</u>	1.04	1.08	1.09	1.16	0.902	0.951
electricity/W/short	<u>1.46</u> ± 0.010	1.48	1.50	1.45	1.86	1.45	<u>1.79</u>	1.92	2.52	1.49	1.54
ett1/15T/long	1.05 ± 0.009	1.14	1.19	<u>1.11</u>	1.32	<u>1.11</u>	1.40	1.12	1.20	1.35	1.50
ett1/15T/medium	1.04 ± 0.009	1.06	1.11	1.08	1.27	<u>1.05</u>	1.30	1.24	1.14	1.32	1.36
ett1/15T/short	0.706 ± 0.007	0.680	<u>0.704</u>	0.719	0.875	0.787	0.925	0.825	0.812	0.801	0.872
ett1/D/short	1.71 ± 0.016	<u>1.67</u>	1.70	1.65	1.70	1.77	1.75	1.74	1.96	1.90	1.80
ett1/H/long	1.34 ± 0.030	<u>1.35</u>	1.44	1.51	1.41	1.46	1.45	1.38	1.36	1.43	1.42
ett1/H/medium	1.25 ± 0.017	1.37	1.37	<u>1.31</u>	1.44	1.36	1.34	1.35	1.32	1.37	<u>1.31</u>
ett1/H/short	0.827 ± 0.007	<u>0.828</u>	0.834	0.866	0.938	0.891	0.855	0.885	0.882	0.840	0.898
ett1/W/short	1.72 ± 0.044	1.70	1.70	1.65	1.73	1.58	1.51	<u>1.54</u>	<u>1.54</u>	1.66	1.65
ett2/15T/long	0.932 ± 0.012	<u>0.940</u>	0.991	0.941	1.03	0.958	1.14	1.30	0.986	1.14	1.11
ett2/15T/medium	0.910 ± 0.010	<u>0.922</u>	0.987	0.938	1.01	0.939	1.06	1.10	0.987	1.06	1.02
ett2/15T/short	0.749 ± 0.010	0.766	0.788	0.747	0.898	0.845	1.00	0.959	0.832	0.857	0.885
ett2/D/short	1.28 ± 0.019	1.32	1.22	1.56	1.64	1.54	1.44	1.31	1.56	<u>1.26</u>	1.43
ett2/H/long	1.16 ± 0.037	1.04	<u>1.07</u>	1.13	1.09	1.37	1.28	1.12	1.13	1.12	1.04
ett2/H/medium	<u>1.05</u> ± 0.021	1.03	<u>1.05</u>	<u>1.05</u>	1.12	1.28	1.18	1.03	1.10	1.15	1.14
ett2/H/short	<u>0.742</u> ± 0.006	0.733	0.744	0.755	0.821	0.787	0.783	0.807	0.790	0.781	0.790
ett2/W/short	0.797 ± 0.040	0.739	0.791	1.12	1.13	0.959	1.31	0.851	1.36	<u>0.749</u>	0.807
hierarchical_sales/D/short	0.744 ± 0.002	0.743	0.749	0.752	0.745	0.766	<u>0.745</u>	<u>0.746</u>	0.834	<u>0.774</u>	0.801
hierarchical_sales/W/short	<u>0.721</u> ± 0.001	0.733	0.733	0.703	0.725	0.723	0.749	0.747	1.09	0.764	0.756
hospital/M/short	<u>0.767</u> ± 0.003	0.791	0.801	<u>0.755</u>	0.783	0.753	<u>0.768</u>	<u>0.775</u>	1.05	0.816	0.813

Table 10: MASE scores of different zero-shot models on the GiftEval benchmark evaluation settings (Part 2/2). The models achieving the **best** and second-best scores are highlighted. Results for datasets that are part of the training data for the respective models are shaded in grey, and these results are excluded from the calculation of the best score. We trained TiRex with 6 different seeds and report the observed standard deviation in the plot.

	TiRex	Chronos Bolt B	Chronos Bolt S	TimesFM 2.0	TimesFM 1.0	TabPFN-TS	Moirai L 1.1	Moirai B 1.1	TTM-r2	Chronos B	Chronos S
jena_weather/10T/long	0.641 ± 0.015	0.657	0.703	0.231	1.36	0.657	0.792	0.762	0.649	0.802	0.956
jena_weather/10T/medium	0.610 ± 0.005	0.610	0.646	0.191	1.10	0.625	0.694	0.712	0.656	0.722	0.744
jena_weather/10T/short	0.297 ± 0.006	<u>0.306</u>	0.320	0.091	0.318	0.325	0.338	0.350	0.346	0.366	0.359
jena_weather/D/short	1.02 ± 0.014	1.05	<u>1.03</u>	1.24	1.20	1.23	1.14	1.15	2.53	1.12	1.14
jena_weather/H/long	<u>0.987</u> ± 0.031	1.03	1.06	1.06	1.38	1.10	0.881	1.06	1.07	1.11	1.16
jena_weather/H/medium	0.828 ± 0.023	<u>0.747</u>	0.721	0.864	1.05	0.954	0.891	0.817	0.815	0.883	0.842
jena_weather/H/short	0.516 ± 0.003	0.536	0.540	<u>0.525</u>	0.589	0.595	0.585	0.554	0.575	0.567	0.583
kdd_cup_2018/D/short	1.21 ± 0.009	1.20	1.19	<u>1.21</u>	<u>1.21</u>	1.17	1.20	1.20	1.17	1.37	1.40
kdd_cup_2018/H/long	0.759 ± 0.027	0.684	0.925	<u>1.03</u>	1.09	1.06	0.867	0.960	1.00	1.14	1.24
kdd_cup_2018/H/medium	0.825 ± 0.024	0.700	0.857	1.03	1.14	1.14	0.954	1.05	<u>1.07</u>	1.24	1.34
kdd_cup_2018/H/short	0.657 ± 0.006	0.601	0.667	0.941	<u>1.09</u>	1.10	0.894	0.944	1.01	1.04	1.06
loop_seattle/5T/long	1.02 ± 0.038	1.24	1.19	1.13	1.43	<u>1.05</u>	0.556	0.591	1.11	1.31	1.38
loop_seattle/5T/medium	0.941 ± 0.019	1.14	1.15	1.12	1.49	<u>0.972</u>	0.450	0.523	1.07	1.61	1.61
loop_seattle/5T/short	0.572 ± 0.005	0.628	0.631	<u>0.583</u>	0.836	0.588	0.486	0.536	0.631	0.764	0.768
loop_seattle/D/short	<u>0.878</u> ± 0.005	0.903	0.919	0.859	0.880	0.899	0.916	0.903	1.74	0.912	1.00
loop_seattle/H/long	<u>0.917</u> ± 0.011	0.996	1.08	0.906	1.26	0.922	1.05	1.15	1.11	1.01	1.12
loop_seattle/H/medium	<u>0.944</u> ± 0.012	1.02	1.10	0.934	1.32	0.948	1.00	1.14	1.19	1.05	1.14
loop_seattle/H/short	<u>0.850</u> ± 0.005	0.900	0.915	0.832	1.15	0.912	0.945	1.06	1.08	0.926	0.967
m4_daily/D/short	3.15 ± 0.063	3.20	3.19	3.09	3.27	4.31	4.18	5.37	4.40	3.18	3.16
m4_hourly/H/short	0.719 ± 0.026	0.837	0.866	0.596	0.768	0.780	0.886	0.971	2.78	0.693	0.739
m4_monthly/M/short	0.929 ± 0.004	0.949	0.954	0.600	0.957	0.895	0.977	0.953	<u>1.53</u>	0.973	0.982
m4_quarterly/Q/short	1.18 ± 0.013	1.22	1.25	0.965	1.40	1.17	1.14	1.14	2.03	1.23	1.24
m4_weekly/W/short	1.90 ± 0.029	2.08	2.11	2.22	2.42	2.07	2.58	2.81	3.48	2.08	2.09
m4_yearly/A/short	3.45 ± 0.075	3.51	3.69	2.54	3.35	3.16	<u>2.97</u>	3.01	5.13	3.64	3.74
m_dense/D/short	0.688 ± 0.016	0.716	0.742	<u>0.636</u>	0.702	0.634	0.957	1.10	1.21	0.712	0.834
m_dense/H/long	0.730 ± 0.013	0.938	0.913	0.795	0.787	1.04	0.696	0.734	1.06	0.773	0.737
m_dense/H/medium	0.736 ± 0.016	0.881	0.820	0.771	0.765	1.02	0.684	0.734	1.02	0.757	<u>0.712</u>
m_dense/H/short	0.788 ± 0.009	0.775	0.805	0.848	0.849	0.916	<u>0.777</u>	0.837	1.09	0.800	0.803
restaurant/D/short	0.677 ± 0.002	0.700	0.700	<u>0.692</u>	0.704	0.782	<u>0.715</u>	0.704	0.897	0.728	0.758
saugreen/D/short	3.12 ± 0.108	2.84	<u>2.96</u>	3.34	3.30	3.30	3.29	2.91	4.03	3.29	2.98
saugreen/M/short	0.750 ± 0.020	0.739	<u>0.727</u>	0.836	0.814	0.707	0.756	0.834	0.790	0.854	0.992
saugreen/W/short	1.18 ± 0.028	<u>1.22</u>	1.24	1.95	1.28	1.25	1.38	1.41	1.87	1.35	1.37
solar/10T/long	0.828 ± 0.021	1.07	1.19	1.15	1.58	<u>0.915</u>	1.95	2.02	1.10	1.66	1.98
solar/10T/medium	0.879 ± 0.037	1.03	1.06	1.17	1.38	<u>0.935</u>	1.82	1.89	1.13	1.54	1.79
solar/10T/short	1.05 ± 0.032	<u>0.991</u>	0.947	1.48	1.49	1.08	1.11	1.10	1.18	1.11	1.22
solar/D/short	0.971 ± 0.005	<u>0.982</u>	0.995	0.971	0.990	0.985	0.987	1.02	1.07	1.01	1.08
solar/H/long	0.697 ± 0.024	1.03	<u>0.957</u>	1.27	1.44	0.977	1.02	1.07	1.12	1.07	1.01
solar/H/medium	0.731 ± 0.026	0.931	<u>0.926</u>	0.959	1.04	0.921	0.917	0.892	1.05	<u>0.806</u>	0.815
solar/H/short	0.699 ± 0.019	<u>0.813</u>	0.852	1.02	1.04	0.937	0.875	0.893	0.980	0.827	0.855
solar/W/short	1.13 ± 0.075	<u>0.980</u>	0.991	1.28	1.15	<u>0.878</u>	1.53	1.66	2.88	1.15	0.877
sz_taxi/15T/long	0.509 ± 0.003	0.545	<u>0.538</u>	0.514	0.535	0.560	0.554	0.537	<u>0.531</u>	0.567	0.584
sz_taxi/15T/medium	0.536 ± 0.001	<u>0.559</u>	0.562	0.546	0.558	0.585	0.569	0.558	0.566	0.597	0.618
sz_taxi/15T/short	0.544 ± 0.001	<u>0.548</u>	0.550	0.539	0.558	0.571	0.581	0.576	0.574	0.589	0.598
sz_taxi/H/short	0.563 ± 0.002	<u>0.562</u>	0.567	0.560	0.566	0.582	0.601	0.588	<u>0.597</u>	0.576	0.579
temperature_rain/D/short	1.34 ± 0.003	1.30	1.32	1.43	<u>1.42</u>	1.38	1.20	1.31	1.66	1.41	1.44
us_births/D/short	0.404 ± 0.017	0.485	0.528	<u>0.370</u>	0.552	0.320	0.503	0.509	1.63	0.420	0.436
us_births/M/short	0.808 ± 0.066	0.924	0.756	0.497	0.622	0.588	0.771	0.723	1.32	0.778	0.572
us_births/W/short	1.08 ± 0.032	1.09	1.12	1.10	1.06	<u>0.929</u>	1.47	1.44	1.78	0.932	0.921

Table 11: CRPS scores of different zero-shot models on the GiftEval benchmark evaluation settings (Part 1/2). The models achieving the **best** and **second-best** scores are highlighted. Results for datasets that are part of the training data for the respective models are shaded in grey, and these results are excluded from the calculation of the best score. We trained TiRex with 6 different seeds and report the observed standard deviation in the plot.

	TiRex	Chronos Bolt B	Chronos Bolt S	TimesFM 2.0	TimesFM 1.0	TabPFN-TS	Moirai L 1.1	Moirai B 1.1	TTM-r2	Chronos B	Chronos S
bitbrains_fast_storage/5T/long	0.655 ± 0.028	0.748	0.753	0.908	0.806	0.760	0.716	0.732	0.939	0.711	0.709
bitbrains_fast_storage/5T/medium	0.605 ± 0.016	0.755	0.867	0.881	0.746	0.735	<u>0.636</u>	0.662	0.906	0.804	0.803
bitbrains_fast_storage/5T/short	0.408 ± 0.005	0.454	0.435	0.447	0.476	0.456	<u>0.412</u>	0.413	0.596	0.463	0.446
bitbrains_fast_storage/H/short	0.699 ± 0.013	0.774	0.589	0.688	0.699	<u>0.591</u>	0.646	0.613	0.926	0.622	0.614
bitbrains_rnd/5T/long	0.660 ± 0.065	0.756	0.756	0.706	0.806	0.730	0.678	<u>0.665</u>	0.779	1.05	1.08
bitbrains_rnd/5T/medium	0.594 ± 0.019	<u>0.605</u>	0.792	0.727	0.734	0.710	0.594	0.616	0.835	0.644	0.615
bitbrains_rnd/5T/short	0.403 ± 0.001	0.438	0.453	0.461	0.519	0.455	<u>0.418</u>	0.446	0.605	0.507	0.493
bitbrains_rnd/H/short	0.631 ± 0.013	0.624	0.623	0.649	0.654	0.637	0.566	<u>0.580</u>	1.06	0.665	0.614
bitzotobs_application/10S/long	0.053 ± 0.004	0.109	0.092	<u>0.057</u>	0.128	0.088	0.094	0.120	0.144	0.093	0.093
bitzotobs_application/10S/medium	<u>0.041</u> ± 0.003	0.104	0.085	0.033	0.136	0.070	0.084	0.104	0.126	0.117	0.078
bitzotobs_application/10S/short	0.013 ± 0.001	0.054	0.035	<u>0.014</u>	0.056	0.031	0.038	0.033	0.058	0.031	0.031
bitzotobs_12c/5T/long	0.581 ± 0.032	0.738	0.790	0.748	0.734	<u>0.511</u>	0.508	0.554	0.785	0.722	0.743
bitzotobs_12c/5T/medium	<u>0.366</u> ± 0.015	0.445	0.462	0.529	0.449	0.345	0.410	0.380	0.540	0.484	0.465
bitzotobs_12c/5T/short	0.078 ± 0.002	<u>0.074</u>	0.073	0.084	0.080	0.099	0.079	0.078	0.107	0.084	0.087
bitzotobs_12c/H/long	0.276 ± 0.010	<u>0.278</u>	0.295	0.728	0.724	0.440	0.600	0.495	0.751	0.738	0.780
bitzotobs_12c/H/medium	0.253 ± 0.008	<u>0.254</u>	0.285	0.640	0.856	0.380	0.619	0.688	0.782	0.793	0.780
bitzotobs_12c/H/short	0.227 ± 0.011	0.189	<u>0.204</u>	0.345	0.485	0.290	0.559	0.493	0.549	0.469	0.428
bitzotobs_service/10S/long	0.054 ± 0.002	0.113	0.096	<u>0.062</u>	0.137	0.091	0.104	0.115	0.140	0.094	0.093
bitzotobs_service/10S/medium	0.034 ± 0.002	0.096	0.082	<u>0.038</u>	0.109	0.067	0.069	0.090	0.117	0.073	0.068
bitzotobs_service/10S/short	0.013 ± 0.000	0.051	0.032	<u>0.015</u>	0.051	0.031	0.032	0.042	0.053	0.027	0.027
car_parts/M/short	0.990 ± 0.010	0.995	1.01	1.05	1.02	0.955	1.18	0.999	2.29	1.07	1.03
covid_deaths/D/short	0.037 ± 0.004	0.047	0.043	0.062	0.204	<u>0.040</u>	<u>0.046</u>	<u>0.044</u>	0.123	0.045	0.061
electricity/15T/long	0.075 ± 0.001	0.084	0.086	0.083	0.137	<u>0.089</u>	0.099	0.115	0.143	0.095	0.098
electricity/15T/medium	0.075 ± 0.001	0.083	0.087	0.080	0.138	<u>0.092</u>	0.103	0.106	0.142	0.095	0.096
electricity/15T/short	0.082 ± 0.000	0.082	0.082	0.079	0.130	<u>0.104</u>	0.128	0.120	0.152	0.092	0.099
electricity/D/short	<u>0.056</u> ± 0.001	0.055	0.058	0.060	0.077	0.060	0.069	0.061	0.093	0.061	0.071
electricity/H/long	<u>0.092</u> ± 0.003	0.098	0.102	<u>0.089</u>	0.101	0.112	0.103	0.086	0.128	0.105	0.107
electricity/H/medium	0.078 ± 0.002	0.081	0.084	0.073	<u>0.082</u>	0.091	0.087	<u>0.082</u>	0.109	0.087	0.088
electricity/H/short	0.061 ± 0.001	0.064	0.067	0.054	<u>0.064</u>	0.072	0.077	0.075	0.097	0.064	0.070
electricity/W/short	0.046 ± 0.001	0.047	0.048	0.049	0.088	<u>0.051</u>	0.062	0.077	0.159	0.049	0.052
ett1/15T/long	0.246 ± 0.003	0.298	0.296	0.283	0.358	<u>0.260</u>	0.358	0.273	0.352	0.400	0.450
ett1/15T/medium	<u>0.251</u> ± 0.002	0.281	0.288	0.278	0.329	0.248	0.342	0.324	0.333	0.379	0.390
ett1/15T/short	<u>0.161</u> ± 0.003	0.158	0.169	0.168	0.193	0.183	0.226	0.193	0.235	0.198	0.217
ett1/D/short	0.282 ± 0.004	0.287	0.283	<u>0.281</u>	0.280	0.292	0.286	0.301	0.416	0.387	0.360
ett1/H/long	0.263 ± 0.004	0.311	0.337	0.310	0.317	0.290	0.296	<u>0.287</u>	0.342	0.350	0.360
ett1/H/medium	0.253 ± 0.002	0.303	0.295	0.282	0.304	0.276	<u>0.270</u>	0.282	0.339	0.330	0.327
ett1/H/short	0.179 ± 0.002	<u>0.181</u>	0.189	0.192	0.209	0.194	0.189	0.197	0.250	0.194	0.222
ett1/W/short	0.306 ± 0.009	0.296	0.293	0.272	0.307	0.256	<u>0.260</u>	0.261	0.448	0.312	0.317
ett2/15T/long	0.097 ± 0.001	0.111	0.118	0.106	0.119	<u>0.101</u>	0.115	0.137	0.126	0.134	0.129
ett2/15T/medium	0.093 ± 0.001	0.110	0.119	0.105	0.112	<u>0.098</u>	0.105	0.109	0.128	0.122	0.117
ett2/15T/short	<u>0.066</u> ± 0.001	0.067	0.070	0.065	0.077	0.073	0.080	0.078	0.093	0.071	0.073
ett2/D/short	<u>0.092</u> ± 0.001	0.094	0.091	0.108	0.113	0.129	0.094	0.095	0.119	<u>0.092</u>	0.097
ett2/H/long	<u>0.116</u> ± 0.004	0.117	0.121	0.125	0.125	0.136	0.125	0.110	0.144	0.136	0.122
ett2/H/medium	<u>0.106</u> ± 0.002	0.115	0.118	0.110	0.126	0.128	0.118	0.100	0.139	0.132	0.136
ett2/H/short	<u>0.065</u> ± 0.001	0.063	<u>0.065</u>	0.066	0.074	0.070	0.069	0.072	0.088	0.071	0.072
ett2/W/short	0.088 ± 0.002	0.088	0.094	0.110	0.111	0.120	0.109	<u>0.087</u>	0.200	0.077	0.077
hierarchical_sales/D/short	0.572 ± 0.002	0.576	0.582	0.576	<u>0.573</u>	0.593	0.580	0.575	0.792	0.600	0.619
hierarchical_sales/W/short	0.349 ± 0.003	0.353	0.354	0.330	<u>0.343</u>	<u>0.342</u>	0.359	0.357	0.725	0.367	0.367
hospital/M/short	<u>0.052</u> ± 0.000	0.057	0.058	0.050	<u>0.052</u>	0.050	0.051	0.051	0.123	0.056	0.056

Table 12: CRPS scores of different zero-shot models on the GiftEval benchmark evaluation settings (Part 2/2). The models achieving the **best** and second-best scores are highlighted. Results for datasets that are part of the training data for the respective models are shaded in grey, and these results are excluded from the calculation of the best score. We trained TiRex with 6 different seeds and report the observed standard deviation in the plot.

	TiRex	Chronos Bolt B	Chronos Bolt S	TimesFM 2.0	TimesFM 1.0	TabPFN-TS	Moirai L 1.1	Moirai B 1.1	TTM-r2	Chronos B	Chronos S
jena_weather/10T/long	0.053 ± 0.001	0.064	0.063	0.035	0.069	0.055	0.077	0.070	0.068	0.080	0.096
jena_weather/10T/medium	0.051 ± 0.001	0.057	0.060	0.031	0.067	0.057	0.072	0.068	0.069	0.076	0.089
jena_weather/10T/short	0.030 ± 0.001	0.033	0.037	0.016	0.036	0.035	0.051	0.053	0.045	0.044	0.047
jena_weather/D/short	0.046 ± 0.001	0.045	0.047	0.058	0.059	0.047	0.051	0.050	0.124	0.049	0.051
jena_weather/H/long	0.057 ± 0.002	0.062	0.068	0.068	0.089	0.066	0.061	0.065	0.084	0.074	0.072
jena_weather/H/medium	0.051 ± 0.002	0.054	0.058	0.066	0.065	0.060	0.058	0.057	0.073	0.070	0.069
jena_weather/H/short	0.041 ± 0.000	0.042	0.043	0.045	0.048	0.043	0.045	0.044	0.060	0.046	0.047
kdd_cup_2018/D/short	0.381 ± 0.005	0.372	0.373	0.378	0.380	0.359	0.381	0.376	0.452	0.503	0.512
kdd_cup_2018/H/long	0.341 ± 0.014	0.300	0.419	0.518	0.537	0.462	0.378	0.418	0.542	0.624	0.712
kdd_cup_2018/H/medium	0.337 ± 0.011	0.301	0.364	0.466	0.493	0.462	0.387	0.441	0.532	0.664	0.706
kdd_cup_2018/H/short	0.270 ± 0.004	0.246	0.267	0.376	0.446	0.437	0.362	0.389	0.514	0.459	0.459
loop_seattle/5T/long	0.090 ± 0.004	0.129	0.125	0.114	0.148	0.094	0.049	0.052	0.125	0.143	0.150
loop_seattle/5T/medium	0.083 ± 0.002	0.116	0.119	0.110	0.151	0.087	0.038	0.045	0.121	0.176	0.175
loop_seattle/5T/short	0.049 ± 0.000	0.055	0.055	0.051	0.075	0.052	0.041	0.046	0.068	0.070	0.070
loop_seattle/D/short	0.042 ± 0.000	0.044	0.045	0.041	0.043	0.044	0.045	0.044	0.101	0.045	0.048
loop_seattle/H/long	0.063 ± 0.001	0.076	0.082	0.066	0.097	0.063	0.074	0.080	0.097	0.082	0.089
loop_seattle/H/medium	0.065 ± 0.001	0.076	0.082	0.067	0.100	0.065	0.070	0.080	0.104	0.084	0.088
loop_seattle/H/short	0.059 ± 0.000	0.065	0.066	0.059	0.082	0.064	0.066	0.074	0.095	0.066	0.069
m4_daily/D/short	0.021 ± 0.000	0.021	0.021	0.021	0.021	0.024	0.030	0.040	0.035	0.022	0.021
m4_hourly/H/short	0.021 ± 0.000	0.025	0.020	0.011	0.021	0.028	0.020	0.022	0.040	0.024	0.025
m4_monthly/M/short	0.093 ± 0.000	0.094	0.094	0.067	0.097	0.088	0.095	0.094	0.177	0.104	0.103
m4_quarterly/Q/short	0.074 ± 0.000	0.077	0.078	0.062	0.085	0.075	0.073	0.073	0.139	0.083	0.084
m4_weekly/W/short	0.035 ± 0.001	0.038	0.038	0.042	0.041	0.036	0.046	0.048	0.069	0.037	0.040
m4_yearly/A/short	0.119 ± 0.002	0.121	0.128	0.091	0.117	0.113	0.104	0.105	0.197	0.135	0.139
m_dense/D/short	0.066 ± 0.002	0.069	0.072	0.060	0.070	0.057	0.095	0.104	0.151	0.075	0.087
m_dense/H/long	0.122 ± 0.003	0.170	0.146	0.127	0.135	0.164	0.114	0.122	0.222	0.135	0.133
m_dense/H/medium	0.121 ± 0.002	0.157	0.134	0.127	0.132	0.159	0.112	0.123	0.213	0.136	0.128
m_dense/H/short	0.130 ± 0.001	0.125	0.133	0.139	0.140	0.154	0.128	0.140	0.225	0.137	0.140
restaurant/D/short	0.254 ± 0.001	0.264	0.264	0.261	0.265	0.297	0.270	0.266	0.438	0.279	0.292
saugreen/D/short	0.382 ± 0.014	0.338	0.354	0.408	0.417	0.384	0.406	0.354	0.589	0.432	0.387
saugreen/M/short	0.303 ± 0.009	0.296	0.293	0.342	0.328	0.278	0.324	0.348	0.405	0.408	0.464
saugreen/W/short	0.353 ± 0.009	0.363	0.372	0.601	0.382	0.380	0.430	0.423	0.696	0.473	0.482
solar/10T/long	0.328 ± 0.008	0.443	0.497	0.498	0.703	0.352	0.771	0.903	0.545	0.748	0.901
solar/10T/medium	0.354 ± 0.016	0.436	0.453	0.516	0.623	0.359	0.747	0.832	0.573	0.686	0.796
solar/10T/short	0.542 ± 0.017	0.511	0.498	0.804	0.871	0.545	0.596	0.614	0.785	0.579	0.635
solar/D/short	0.281 ± 0.002	0.287	0.286	0.278	0.288	0.269	0.292	0.295	0.396	0.326	0.337
solar/H/long	0.243 ± 0.008	0.405	0.373	0.493	0.572	0.324	0.347	0.360	0.512	0.464	0.441
solar/H/medium	0.260 ± 0.010	0.368	0.356	0.376	0.425	0.324	0.346	0.331	0.493	0.356	0.361
solar/H/short	0.259 ± 0.009	0.298	0.303	0.406	0.403	0.358	0.333	0.338	0.468	0.334	0.345
solar/W/short	0.154 ± 0.008	0.133	0.136	0.171	0.157	0.124	0.213	0.235	0.531	0.161	0.124
sz_taxi/15T/long	0.197 ± 0.001	0.248	0.245	0.227	0.238	0.248	0.213	0.209	0.260	0.265	0.275
sz_taxi/15T/medium	0.202 ± 0.001	0.244	0.246	0.229	0.233	0.245	0.215	0.211	0.270	0.268	0.279
sz_taxi/15T/short	0.200 ± 0.000	0.202	0.203	0.199	0.206	0.215	0.215	0.213	0.268	0.236	0.241
sz_taxi/H/short	0.136 ± 0.000	0.136	0.137	0.135	0.137	0.144	0.146	0.143	0.183	0.149	0.149
temperature_rain/D/short	0.550 ± 0.002	0.538	0.544	0.586	0.581	0.565	0.479	0.535	0.791	0.610	0.627
us_births/D/short	0.021 ± 0.001	0.026	0.028	0.019	0.029	0.018	0.027	0.027	0.104	0.022	0.023
us_births/M/short	0.017 ± 0.002	0.019	0.016	0.011	0.013	0.013	0.016	0.015	0.036	0.018	0.013
us_births/W/short	0.013 ± 0.000	0.013	0.013	0.013	0.013	0.011	0.018	0.017	0.027	0.011	0.011

Table 13: MASE scores of TiRex compared with various task-specific and local models on the GiftEval benchmark evaluation settings (Part 1/2). Models achieving the **best** and **second-best** scores are highlighted, while the grey shade indicates results on datasets TiRex trained on. We trained TiRex with 6 different seeds and report the observed standard deviation in the plot.

	TiRex	DeepAR	PatchTST	DLinear	TFT	N-Beats	Auto ARIMA	Auto Theta	Seas. Naive
bitbrains_fast_storage/5T/long	0.916 ± 0.006	7.33	<u>1.14</u>	3.47	1.21	1.40	<u>1.14</u>	1.61	<u>1.14</u>
bitbrains_fast_storage/5T/medium	1.00 ± 0.011	8.50	<u>1.20</u>	3.33	1.38	1.60	<u>1.22</u>	1.42	<u>1.22</u>
bitbrains_fast_storage/5T/short	0.692 ± 0.007	<u>0.945</u>	0.973	1.48	0.996	1.09	1.14	1.15	1.14
bitbrains_fast_storage/H/short	1.06 ± 0.013	6.06	1.34	2.65	1.73	1.37	1.43	1.35	<u>1.30</u>
bitbrains_rnd/5T/long	3.35 ± 0.013	4.44	3.72	6.35	3.71	3.95	<u>3.50</u>	4.11	<u>3.50</u>
bitbrains_rnd/5T/medium	4.40 ± 0.007	4.89	4.65	7.08	4.81	4.79	<u>4.54</u>	4.88	<u>4.54</u>
bitbrains_rnd/5T/short	1.66 ± 0.004	2.10	1.98	2.63	2.27	2.18	<u>1.97</u>	2.07	<u>1.97</u>
bitbrains_rnd/H/short	<u>5.84</u> ± 0.011	6.06	6.11	8.50	6.19	6.16	6.08	5.75	6.04
bizitobs_application/10S/long	3.67 ± 0.069	4.47	<u>3.19</u>	4.25	14.8	3.83	36400	2.93	36400
bizitobs_application/10S/medium	2.85 ± 0.057	3.22	2.77	3.88	13.8	<u>2.57</u>	2.69	1.78	2.69
bizitobs_application/10S/short	<u>1.40</u> ± 0.112	4.16	2.24	7.65	9.11	2.57	2.24	1.11	2.24
bizitobs_l2c/5T/long	<u>1.19</u> ± 0.040	1.32	0.686	1.12	1.06	<u>0.968</u>	1.45	1.24	1.45
bizitobs_l2c/5T/medium	0.849 ± 0.028	1.21	<u>0.787</u>	0.894	0.786	0.935	1.24	0.868	1.24
bizitobs_l2c/5T/short	0.290 ± 0.005	0.613	<u>0.266</u>	0.243	0.278	0.297	0.986	0.292	0.986
bizitobs_l2c/H/long	0.590 ± 0.022	0.727	0.617	0.744	<u>0.599</u>	0.811	1.54	1.41	4.04
bizitobs_l2c/H/medium	0.525 ± 0.020	0.737	<u>0.537</u>	0.676	0.693	0.701	1.56	1.65	1.65
bizitobs_l2c/H/short	<u>0.528</u> ± 0.021	1.50	0.495	0.640	0.862	0.536	1.25	1.19	1.21
bizitobs_service/10S/long	<u>1.57</u> ± 0.057	3.96	1.69	2.29	1.75	2.62	1.37	1.62	1.37
bizitobs_service/10S/medium	<u>1.32</u> ± 0.058	2.17	1.49	2.23	1.68	2.59	<u>1.32</u>	1.06	<u>1.32</u>
bizitobs_service/10S/short	<u>0.884</u> ± 0.052	2.67	1.24	1.87	2.15	1.12	1.23	0.791	1.23
car_parts/M/short	0.838 ± 0.004	0.835	0.797	0.997	<u>0.807</u>	0.810	0.958	1.23	1.20
covid_deaths/D/short	39.5 ± 0.803	50.7	37.7	33.2	32.9	<u>32.8</u>	31.4	45.4	46.9
electricity/15T/long	0.891 ± 0.008	2.28	0.960	1.24	<u>1.03</u>	1.15	1.16	1.50	1.16
electricity/15T/medium	0.841 ± 0.006	1.39	0.977	1.31	<u>1.11</u>	1.62	1.15	1.43	1.15
electricity/15T/short	0.945 ± 0.008	1.67	<u>1.47</u>	1.64	2.07	1.69	1.72	1.35	1.72
electricity/D/short	1.43 ± 0.010	1.89	1.85	3.56	1.86	1.85	<u>1.82</u>	1.88	1.99
electricity/H/long	<u>1.21</u> ± 0.018	2.67	1.39	2.21	<u>1.41</u>	1.42	1.52	2.05	1.52
electricity/H/medium	1.08 ± 0.010	6.76	1.16	2.26	<u>1.31</u>	1.35	1.39	1.78	1.39
electricity/H/short	0.869 ± 0.009	<u>1.23</u>	1.08	1.31	1.29	1.44	1.36	1.74	1.36
electricity/W/short	1.46 ± 0.010	2.25	<u>1.96</u>	1.84	2.10	2.10	2.09	2.14	2.09
ett1/15T/long	1.05 ± 0.009	9.34	<u>1.10</u>	1.19	1.34	1.42	1.19	1.76	1.19
ett1/15T/medium	1.04 ± 0.009	1.35	<u>1.08</u>	1.20	<u>1.08</u>	1.41	1.19	1.25	1.19
ett1/15T/short	0.706 ± 0.007	1.44	0.835	<u>0.804</u>	1.05	0.870	0.934	0.863	0.934
ett1/D/short	1.71 ± 0.016	<u>1.69</u>	1.68	1.98	1.86	2.04	1.85	1.75	1.78
ett1/H/long	1.34 ± 0.030	2.68	1.47	<u>1.46</u>	1.55	1.96	1.65	2.51	1.48
ett1/H/medium	1.25 ± 0.017	3.12	<u>1.39</u>	1.66	1.58	1.67	1.57	1.84	1.57
ett1/H/short	0.827 ± 0.007	1.06	<u>0.893</u>	0.945	0.947	0.930	0.995	1.28	0.977
ett1/W/short	1.72 ± 0.044	4.16	1.89	2.16	1.61	<u>1.63</u>	1.99	1.89	1.77
ett2/15T/long	0.932 ± 0.012	3.70	<u>0.961</u>	1.10	1.15	0.980	1.01	1.10	1.01
ett2/15T/medium	0.910 ± 0.010	3.27	<u>0.933</u>	1.21	1.10	1.09	1.05	1.04	1.05
ett2/15T/short	0.749 ± 0.010	4.11	0.879	0.937	1.06	1.01	1.07	<u>0.832</u>	1.07
ett2/D/short	1.28 ± 0.019	3.64	2.17	3.25	<u>1.31</u>	1.54	1.45	1.85	1.39
ett2/H/long	<u>1.16</u> ± 0.037	2.49	1.43	1.58	1.45	1.26	1.28	1.46	1.13
ett2/H/medium	1.05 ± 0.021	2.52	1.27	1.36	1.32	1.05	1.46	1.30	<u>1.24</u>
ett2/H/short	0.742 ± 0.006	1.48	0.858	<u>0.817</u>	0.956	0.819	0.952	1.02	0.923
ett2/W/short	<u>0.797</u> ± 0.040	7.17	1.49	1.93	1.60	2.69	1.13	1.41	0.779
hierarchical_sales/D/short	0.744 ± 0.002	0.757	<u>0.756</u>	0.860	0.771	0.773	0.813	0.932	1.13
hierarchical_sales/W/short	0.721 ± 0.001	0.781	<u>0.771</u>	0.993	0.793	0.778	0.850	0.849	1.03
hospital/M/short	<u>0.767</u> ± 0.003	0.834	0.820	0.811	0.833	0.771	0.826	0.761	0.921

Table 14: MASE scores of TiRex compared with various task-specific and local models on the GiftEval benchmark evaluation settings (Part 2/2). Models achieving the **best** and **second-best** scores are highlighted, while the grey shade indicates results on datasets TiRex trained on. We trained TiRex with 6 different seeds and report the observed standard deviation in the plot.

	TiRex	DeepAR	PatchTST	DLInear	TFT	N-Beats	Auto ARIMA	Auto Theta	Seas. Naive
jena_weather/10T/long	0.641 ± 0.015	3.15	1.07	0.912	<u>0.741</u>	0.855	0.761	0.990	0.761
jena_weather/10T/medium	0.610 ± 0.005	1.20	0.943	1.17	0.737	0.749	<u>0.716</u>	0.806	<u>0.716</u>
jena_weather/10T/short	0.297 ± 0.006	0.574	0.552	1.96	0.450	0.527	0.743	<u>0.368</u>	0.743
jena_weather/D/short	1.02 ± 0.014	<u>1.30</u>	1.39	1.60	1.80	1.83	1.45	<u>1.60</u>	1.57
jena_weather/H/long	0.987 ± 0.031	6.89	1.31	1.90	1.15	<u>1.13</u>	1.98	2.64	1.27
jena_weather/H/medium	0.828 ± 0.023	1.30	1.09	0.997	0.939	0.902	1.45	1.36	<u>0.889</u>
jena_weather/H/short	0.516 ± 0.003	18.8	0.641	0.982	<u>0.634</u>	0.763	1.08	0.878	<u>0.723</u>
kdd_cup_2018/D/short	1.21 ± 0.009	1.23	1.22	1.23	<u>1.21</u>	1.35	1.18	1.38	1.50
kdd_cup_2018/H/long	0.759 ± 0.027	3.34	1.02	<u>1.09</u>	1.11	1.18	1.18	1.37	1.34
kdd_cup_2018/H/medium	0.825 ± 0.024	1.17	1.05	<u>1.12</u>	1.16	1.29	1.42	1.33	1.43
kdd_cup_2018/H/short	0.657 ± 0.006	1.28	1.12	<u>1.13</u>	1.15	1.30	1.34	1.27	1.34
loop_seattle/5T/long	1.02 ± 0.038	1.96	1.06	1.17	0.977	1.05	1.25	1.44	1.25
loop_seattle/5T/medium	0.941 ± 0.019	1.27	1.05	1.12	<u>1.01</u>	1.05	1.15	2.06	1.15
loop_seattle/5T/short	0.572 ± 0.005	0.803	0.744	0.895	<u>0.731</u>	0.735	0.762	0.780	0.762
loop_seattle/D/short	0.878 ± 0.005	1.08	0.934	0.900	0.973	<u>0.898</u>	1.49	1.39	1.73
loop_seattle/H/long	0.917 ± 0.011	0.985	0.979	1.03	0.972	<u>0.932</u>	2.59	2.02	1.55
loop_seattle/H/medium	0.944 ± 0.012	1.03	1.03	1.20	<u>0.971</u>	1.03	2.00	1.61	1.48
loop_seattle/H/short	0.850 ± 0.005	<u>0.941</u>	1.07	1.13	1.04	1.03	1.29	1.40	1.29
m4_daily/D/short	3.15 ± 0.063	4.58	3.22	3.42	3.29	3.35	<u>3.26</u>	3.34	3.28
m4_hourly/H/short	0.719 ± 0.026	3.53	1.40	1.69	2.47	1.34	1.03	2.46	<u>1.19</u>
m4_monthly/M/short	0.929 ± 0.004	3.18	1.06	1.13	1.21	1.05	<u>0.976</u>	0.966	1.26
m4_quarterly/Q/short	1.18 ± 0.013	1.44	1.32	1.46	1.30	1.21	1.28	<u>1.19</u>	1.60
m4_weekly/W/short	1.90 ± 0.029	4.62	<u>2.34</u>	4.64	2.68	1.97	2.36	2.66	2.78
m4_yearly/A/short	3.45 ± 0.075	3.40	3.29	4.16	3.09	3.15	3.71	<u>3.11</u>	3.97
m_dense/D/short	0.688 ± 0.016	0.793	0.732	1.01	0.799	<u>0.706</u>	1.34	1.22	1.67
m_dense/H/long	<u>0.730</u> ± 0.013	0.805	0.738	1.24	0.723	1.18	1.21	2.29	1.48
m_dense/H/medium	<u>0.736</u> ± 0.016	0.738	0.757	0.930	0.732	0.890	1.27	1.74	1.57
m_dense/H/short	0.788 ± 0.009	<u>0.795</u>	1.03	1.04	0.878	0.915	1.49	1.69	1.49
restaurant/D/short	0.677 ± 0.002	0.713	<u>0.690</u>	0.706	0.750	0.712	0.929	0.843	1.01
saugeen/D/short	3.12 ± 0.108	4.31	3.28	4.20	<u>3.22</u>	3.28	3.74	3.60	3.41
saugeen/M/short	<u>0.750</u> ± 0.020	1.63	0.893	0.955	0.865	0.758	0.725	0.912	0.976
saugeen/W/short	1.18 ± 0.028	<u>1.31</u>	1.55	1.81	1.55	1.54	1.55	2.12	1.99
solar/10T/long	0.828 ± 0.021	1.28	0.912	1.18	1.00	2.03	<u>0.871</u>	4.53	<u>0.871</u>
solar/10T/medium	0.879 ± 0.037	1.21	<u>0.913</u>	1.08	0.931	1.98	0.927	2.69	0.927
solar/10T/short	<u>1.05</u> ± 0.032	1.47	2.20	1.24	1.11	0.848	1.11	1.80	1.11
solar/D/short	<u>0.971</u> ± 0.005	2.49	0.962	1.03	0.999	1.21	1.01	1.05	1.16
solar/H/long	0.697 ± 0.024	<u>0.972</u>	0.978	1.35	1.12	2.21	0.995	5.24	1.07
solar/H/medium	0.731 ± 0.026	0.992	0.965	1.17	0.884	2.12	<u>0.848</u>	2.87	0.935
solar/H/short	0.699 ± 0.019	1.02	0.954	1.06	0.960	1.04	<u>0.952</u>	2.05	<u>0.952</u>
solar/W/short	1.13 ± 0.075	1.69	<u>1.10</u>	1.13	0.691	2.33	1.12	1.15	1.47
sz_taxi/15T/long	0.509 ± 0.003	0.733	0.761	0.841	<u>0.535</u>	0.666	0.598	0.759	0.691
sz_taxi/15T/medium	0.536 ± 0.001	0.558	0.588	0.629	<u>0.548</u>	0.662	0.632	0.716	0.713
sz_taxi/15T/short	0.544 ± 0.001	0.602	<u>0.560</u>	0.582	0.603	0.604	0.764	0.649	0.764
sz_taxi/H/short	0.563 ± 0.002	<u>0.576</u>	0.591	0.667	0.595	0.624	0.624	0.691	0.738
temperature_rain/D/short	1.34 ± 0.003	1.72	<u>1.51</u>	1.83	1.44	1.90	1.71	1.93	2.01
us_births/D/short	0.404 ± 0.017	0.535	0.487	0.645	0.315	0.456	1.58	1.63	1.86
us_births/M/short	0.808 ± 0.066	<u>0.760</u>	0.782	1.17	0.871	0.928	0.466	0.883	0.761
us_births/W/short	1.08 ± 0.032	1.45	<u>1.23</u>	1.46	1.59	1.40	1.48	1.49	1.56

Table 15: CRPS scores of TiRex compared with various task-specific and local models on the [GiftEval](#) benchmark evaluation settings (Part 1/2). Models achieving the **best** and **second-best** scores are highlighted, while the grey shade indicates results on datasets TiRex trained on. We trained TiRex with 6 different seeds and report the observed standard deviation in the plot.

	TiRex	DeepAR	PatchTST	DLinear	TFT	N-Beats	Auto ARIMA	Auto Theta	Seas. Naive
bitbrains_fast_storage/5T/long	0.655 ± 0.028	1.01	<u>0.669</u>	1.33	0.734	0.791	1.29	1.36	1.29
bitbrains_fast_storage/5T/medium	0.605 ± 0.016	0.990	<u>0.642</u>	0.967	<u>0.610</u>	0.841	1.27	1.45	1.27
bitbrains_fast_storage/5T/short	0.408 ± 0.005	0.493	0.471	0.577	<u>0.451</u>	0.622	1.21	0.731	1.21
bitbrains_fast_storage/H/short	0.699 ± 0.013	0.778	0.549	0.803	<u>0.595</u>	0.812	0.844	1.15	1.08
bitbrains_rnd/5T/long	<u>0.660</u> ± 0.065	0.672	0.664	1.30	0.624	1.06	1.29	1.60	1.29
bitbrains_rnd/5T/medium	0.594 ± 0.019	0.647	<u>0.620</u>	1.01	0.628	0.699	1.26	1.47	1.26
bitbrains_rnd/5T/short	0.403 ± 0.001	0.557	<u>0.474</u>	0.571	0.486	0.656	1.10	0.741	1.10
bitbrains_rnd/H/short	0.631 ± 0.013	0.585	<u>0.603</u>	1.07	0.650	0.715	0.874	1.38	1.30
bizitobs_application/10S/long	<u>0.053</u> ± 0.004	0.083	0.054	0.070	0.056	0.062	0.973	0.035	0.973
bizitobs_application/10S/medium	<u>0.041</u> ± 0.003	0.053	0.047	0.056	0.047	0.047	0.042	0.024	0.042
bizitobs_application/10S/short	<u>0.013</u> ± 0.001	0.064	0.022	0.079	0.090	0.043	0.035	0.010	0.035
bizitobs_12c/5T/long	0.581 ± 0.032	0.719	0.324	0.653	<u>0.472</u>	0.546	0.674	0.632	0.674
bizitobs_12c/5T/medium	0.366 ± 0.015	0.589	0.332	0.490	<u>0.346</u>	0.505	0.530	0.415	0.530
bizitobs_12c/5T/short	0.078 ± 0.002	0.179	0.074	0.080	<u>0.077</u>	0.100	0.262	0.080	0.262
bizitobs_12c/H/long	0.276 ± 0.010	0.338	0.291	0.422	<u>0.286</u>	0.479	0.787	0.819	1.82
bizitobs_12c/H/medium	0.253 ± 0.008	0.345	<u>0.263</u>	0.398	0.345	0.420	0.813	0.892	1.42
bizitobs_12c/H/short	<u>0.227</u> ± 0.011	0.789	0.217	0.336	0.401	0.288	0.547	0.507	0.536
bizitobs_service/10S/long	<u>0.054</u> ± 0.002	0.070	0.057	0.067	0.056	0.061	0.056	0.052	0.056
bizitobs_service/10S/medium	<u>0.034</u> ± 0.002	0.044	0.045	0.053	0.044	0.043	0.049	0.027	0.049
bizitobs_service/10S/short	0.013 ± 0.000	0.032	0.025	0.032	0.025	<u>0.021</u>	0.040	0.013	0.040
car_parts/M/short	0.990 ± 0.010	<u>0.953</u>	1.00	1.26	0.890	1.02	1.29	1.34	1.72
covid_deaths/D/short	<u>0.037</u> ± 0.004	0.177	0.067	0.063	<u>0.037</u>	0.071	0.030	0.095	0.125
electricity/15T/long	<u>0.075</u> ± 0.001	0.155	0.081	0.129	<u>0.084</u>	0.123	0.129	0.401	0.129
electricity/15T/medium	<u>0.075</u> ± 0.001	0.119	0.086	0.142	<u>0.094</u>	0.176	0.124	0.328	0.124
electricity/15T/short	<u>0.082</u> ± 0.000	0.152	0.134	0.177	0.184	0.180	0.165	<u>0.140</u>	0.165
electricity/D/short	0.056 ± 0.001	<u>0.078</u>	0.083	0.169	0.084	0.110	0.083	0.088	0.122
electricity/H/long	<u>0.092</u> ± 0.003	0.176	<u>0.104</u>	0.203	0.094	0.126	0.190	0.300	0.190
electricity/H/medium	<u>0.078</u> ± 0.002	0.454	0.081	0.206	<u>0.091</u>	0.115	0.156	0.254	0.156
electricity/H/short	<u>0.061</u> ± 0.001	0.094	0.079	0.112	<u>0.089</u>	0.123	0.109	0.177	0.109
electricity/W/short	<u>0.046</u> ± 0.001	0.092	<u>0.095</u>	0.111	0.107	0.123	0.100	0.101	0.099
ett1/15T/long	0.246 ± 0.003	2.22	<u>0.247</u>	0.343	0.280	0.431	0.396	1.39	0.396
ett1/15T/medium	0.251 ± 0.002	0.315	<u>0.250</u>	0.347	0.247	0.430	0.352	1.13	0.352
ett1/15T/short	0.161 ± 0.003	0.320	<u>0.191</u>	0.233	0.245	0.254	0.241	0.410	0.241
ett1/D/short	<u>0.282</u> ± 0.004	0.293	0.304	0.376	0.330	0.387	0.279	0.341	0.515
ett1/H/long	0.263 ± 0.004	0.469	<u>0.297</u>	0.363	0.313	0.567	0.430	1.94	0.616
ett1/H/medium	0.253 ± 0.002	0.535	<u>0.273</u>	0.455	0.316	0.450	0.384	1.65	0.540
ett1/H/short	0.179 ± 0.002	0.233	<u>0.190</u>	0.256	0.199	0.249	0.223	0.668	0.250
ett1/W/short	<u>0.306</u> ± 0.009	0.686	0.323	0.447	0.406	0.372	0.305	0.319	0.338
ett2/15T/long	0.097 ± 0.001	0.304	<u>0.098</u>	0.141	0.109	0.126	0.165	0.169	0.165
ett2/15T/medium	0.093 ± 0.001	0.258	<u>0.094</u>	0.151	0.104	0.138	0.143	0.150	0.143
ett2/15T/short	0.066 ± 0.001	0.378	<u>0.076</u>	0.102	0.081	0.109	0.096	0.077	0.096
ett2/D/short	0.092 ± 0.001	0.207	0.131	0.218	<u>0.096</u>	0.140	0.125	0.164	0.205
ett2/H/long	0.116 ± 0.004	0.196	<u>0.130</u>	0.165	0.138	0.156	0.272	0.336	0.287
ett2/H/medium	0.106 ± 0.002	0.281	0.125	0.166	<u>0.122</u>	0.130	0.245	0.284	0.241
ett2/H/short	0.065 ± 0.001	0.122	<u>0.074</u>	0.088	0.078	0.091	0.089	0.102	0.094
ett2/W/short	0.088 ± 0.002	0.728	0.142	0.194	0.160	0.294	<u>0.136</u>	0.160	0.169
hierarchical_sales/D/short	0.572 ± 0.002	0.600	<u>0.590</u>	0.817	0.600	0.728	0.735	0.967	2.36
hierarchical_sales/W/short	0.349 ± 0.003	0.379	<u>0.358</u>	0.582	0.382	0.439	0.485	0.474	1.03
hospital/M/short	0.052 ± 0.000	0.062	0.064	0.076	0.058	0.068	0.060	<u>0.055</u>	0.062

Table 16: CRPS scores of TiRex compared with various task-specific and local models on the GiftEval benchmark evaluation settings (Part 2/2). Models achieving the **best** and **second-best** scores are highlighted, while the grey shade indicates results on datasets TiRex trained on. We trained TiRex with 6 different seeds and report the observed standard deviation in the plot.

	TiRex	DeepAR	PatchTST	DLlinear	TFT	N-Beats	Auto ARIMA	Auto Theta	Seas. Naive
jena_weather/10T/long	<u>0.053</u> ± 0.001	0.143	0.066	0.093	0.052	0.134	0.304	0.424	0.304
jena_weather/10T/medium	0.051 ± 0.001	0.073	0.065	0.098	<u>0.052</u>	0.089	0.277	0.350	0.277
jena_weather/10T/short	0.030 ± 0.001	<u>0.063</u>	0.064	0.129	<u>0.069</u>	0.104	0.155	0.130	0.155
jena_weather/D/short	0.046 ± 0.001	<u>0.062</u>	<u>0.053</u>	0.073	0.069	0.193	0.080	0.082	0.297
jena_weather/H/long	0.057 ± 0.002	0.197	<u>0.076</u>	0.139	0.090	0.131	0.230	1.29	0.598
jena_weather/H/medium	0.051 ± 0.002	0.078	<u>0.069</u>	0.093	0.073	0.097	0.211	0.832	0.486
jena_weather/H/short	0.041 ± 0.000	0.699	<u>0.050</u>	0.086	<u>0.048</u>	0.098	0.143	0.296	0.173
kdd_cup_2018/D/short	0.381 ± 0.005	0.383	0.401	0.482	0.380	0.529	0.393	0.459	0.888
kdd_cup_2018/H/long	0.341 ± 0.014	1.09	0.477	0.583	<u>0.503</u>	0.660	1.05	0.970	1.25
kdd_cup_2018/H/medium	0.337 ± 0.011	0.442	0.442	0.548	<u>0.472</u>	0.660	0.851	0.791	0.949
kdd_cup_2018/H/short	0.270 ± 0.004	0.517	0.457	0.581	<u>0.467</u>	0.683	0.559	0.531	0.559
loop_seattle/5T/long	<u>0.090</u> ± 0.004	0.184	0.095	0.131	0.088	0.117	0.137	0.231	0.137
loop_seattle/5T/medium	0.083 ± 0.002	0.118	0.095	0.126	<u>0.092</u>	0.118	0.123	0.240	0.123
loop_seattle/5T/short	0.049 ± 0.000	0.072	0.066	0.099	<u>0.065</u>	0.080	0.081	0.082	0.081
loop_seattle/D/short	0.042 ± 0.000	0.052	<u>0.046</u>	0.053	0.048	0.053	0.078	0.072	0.131
loop_seattle/H/long	0.063 ± 0.001	<u>0.068</u>	0.069	0.088	<u>0.068</u>	0.080	0.193	0.468	0.245
loop_seattle/H/medium	0.065 ± 0.001	0.072	0.071	0.104	<u>0.069</u>	0.088	0.154	0.390	0.206
loop_seattle/H/short	0.059 ± 0.000	<u>0.066</u>	0.076	0.099	0.073	0.090	0.108	0.165	0.108
m4_daily/D/short	0.021 ± 0.000	0.030	0.023	0.029	0.023	0.029	0.023	<u>0.024</u>	0.026
m4_hourly/H/short	0.021 ± 0.000	0.133	<u>0.039</u>	0.055	0.040	0.050	0.034	0.041	0.040
m4_monthly/M/short	0.093 ± 0.000	0.184	<u>0.102</u>	0.129	0.113	0.122	0.098	0.098	0.126
m4_quarterly/Q/short	0.074 ± 0.000	0.083	0.083	0.110	0.083	0.096	0.082	<u>0.079</u>	0.099
m4_weekly/W/short	0.035 ± 0.001	0.062	0.040	0.070	0.049	<u>0.047</u>	0.050	0.053	0.073
m4_yearly/A/short	0.119 ± 0.002	<u>0.113</u>	0.117	0.168	0.110	0.134	0.130	0.115	0.138
m_dense/D/short	0.066 ± 0.002	0.076	<u>0.070</u>	0.123	0.077	0.087	0.135	0.126	0.294
m_dense/H/long	0.122 ± 0.003	0.130	<u>0.120</u>	0.259	0.115	0.243	0.270	1.43	0.552
m_dense/H/medium	0.121 ± 0.002	<u>0.118</u>	0.127	0.191	0.114	0.184	0.255	1.21	0.479
m_dense/H/short	<u>0.130</u> ± 0.001	0.128	0.173	0.214	0.139	0.190	0.281	0.549	0.281
restaurant/D/short	0.254 ± 0.001	0.270	<u>0.262</u>	0.340	0.284	0.342	0.362	0.329	0.907
saugdeen/D/short	0.382 ± 0.014	0.572	<u>0.408</u>	0.613	0.419	0.478	0.564	0.669	0.754
saugdeen/M/short	0.303 ± 0.009	0.689	0.372	0.490	0.340	0.388	<u>0.326</u>	0.373	0.445
saugdeen/W/short	0.353 ± 0.009	<u>0.397</u>	0.484	0.673	0.491	0.574	0.549	0.734	0.855
solar/10T/long	0.328 ± 0.008	0.549	<u>0.339</u>	0.585	0.379	1.01	0.786	6.64	0.786
solar/10T/medium	0.354 ± 0.016	0.485	<u>0.356</u>	0.552	0.362	1.00	0.771	5.67	0.771
solar/10T/short	0.542 ± 0.017	0.933	1.37	0.824	0.618	<u>0.576</u>	0.860	2.36	0.860
solar/D/short	0.281 ± 0.002	0.682	0.287	0.383	0.277	0.450	0.282	0.286	0.757
solar/H/long	0.243 ± 0.008	0.381	<u>0.353</u>	0.612	0.401	1.00	0.607	7.32	1.47
solar/H/medium	0.260 ± 0.010	0.352	0.344	0.552	<u>0.330</u>	1.00	0.557	6.13	1.27
solar/H/short	0.259 ± 0.009	0.389	<u>0.340</u>	0.507	0.367	0.498	0.628	2.33	0.628
solar/W/short	0.154 ± 0.008	0.242	0.162	0.210	0.114	0.432	<u>0.152</u>	0.155	0.236
sz_taxi/15T/long	0.197 ± 0.001	0.286	0.281	0.396	<u>0.241</u>	0.323	0.398	0.629	0.554
sz_taxi/15T/medium	0.202 ± 0.001	0.210	0.220	0.296	<u>0.206</u>	0.314	0.351	0.529	0.454
sz_taxi/15T/short	0.200 ± 0.000	0.219	<u>0.207</u>	0.271	0.222	0.281	0.309	0.288	0.309
sz_taxi/H/short	0.136 ± 0.000	<u>0.139</u>	0.144	0.201	0.144	0.190	0.170	0.232	0.229
temperature_rain/D/short	<u>0.550</u> ± 0.002	0.682	<u>0.644</u>	0.830	0.592	0.840	0.694	0.761	1.63
us_births/D/short	<u>0.021</u> ± 0.001	0.028	0.025	0.041	0.016	0.029	0.074	0.075	0.144
us_births/M/short	<u>0.017</u> ± 0.002	<u>0.016</u>	0.017	0.032	0.021	0.025	0.010	0.019	0.017
us_births/W/short	0.013 ± 0.000	0.017	<u>0.015</u>	0.022	0.019	0.021	0.018	0.018	0.022

Table 17: MASE scores of different zero-shot models on the Chronos-ZS benchmark datasets. The models achieving the **best** and **second-best** scores are highlighted. Results for datasets that are part of the training data for the respective models are shaded in grey, and these results are excluded from the calculation of the best score. We trained TiRex with 6 different seeds and report the observed standard deviation in the plot.

	TiRex	Chronos Bolt B	Chronos Bolt S	TimesFM 2.0	TimesFM 1.0	TabPFN-TS	Moirai L 1.1	Moirai B 1.1	TTM-r2	Chronos B	Chronos S
ETTh	0.793 ± 0.019	0.748	0.793	0.854	0.890	0.903	0.825	0.902	0.973	<u>0.774</u>	0.827
ETTm	0.641 ± 0.006	0.633	<u>0.621</u>	0.620	1.04	0.806	0.755	0.826	0.781	0.803	0.718
australian electricity	1.06 ± 0.096	0.740	<u>0.813</u>	1.32	1.63	0.997	<u>0.930</u>	<u>1.25</u>	<u>1.22</u>	1.11	1.28
car parts	0.838 ± 0.004	<u>0.855</u>	0.858	0.986	0.901	0.838	<u>0.846</u>	<u>0.863</u>	1.16	0.889	0.875
cif 2016	<u>0.923</u> ± 0.005	0.999	1.02	0.949	1.04	0.894	1.03	1.06	1.61	0.985	0.996
covid deaths	39.5 ± 0.803	38.9	36.5	42.2	55.6	<u>37.8</u>	<u>32.1</u>	<u>34.3</u>	49.5	43.6	42.6
dominick	0.797 ± 0.004	0.856	0.871	0.935	1.13	0.864	0.830	0.828	1.31	0.824	<u>0.812</u>
ercot	0.630 ± 0.040	0.693	0.756	0.688	0.589	0.603	<u>0.568</u>	<u>0.569</u>	1.03	0.463	0.571
exchange rate	2.20 ± 0.157	<u>1.71</u>	1.77	1.98	3.34	1.44	1.74	1.81	2.01	2.18	1.78
fred md	<u>0.451</u> ± 0.023	0.646	0.612	0.498	0.650	0.530	<u>0.564</u>	<u>0.572</u>	0.698	0.445	0.445
hospital	0.767 ± 0.003	0.791	0.801	<u>0.755</u>	0.783	0.686	0.830	0.820	<u>0.843</u>	0.812	0.815
m1 monthly	<u>1.05</u> ± 0.008	1.10	1.13	<u>1.05</u>	1.07	1.04	1.14	1.14	1.47	1.12	1.16
m1 quarterly	1.69 ± 0.011	1.77	1.84	1.71	<u>1.67</u>	1.66	1.79	1.64	2.12	1.76	1.81
m1 yearly	3.67 ± 0.095	4.40	5.10	<u>3.60</u>	4.00	3.59	3.52	3.61	5.78	4.48	4.90
m3 monthly	0.847 ± 0.009	0.851	0.869	0.832	0.935	<u>0.845</u>	0.902	0.897	1.23	0.863	0.893
m3 quarterly	1.17 ± 0.011	1.29	1.33	1.20	<u>1.15</u>	1.10	1.12	1.15	1.72	1.18	1.29
m3 yearly	2.76 ± 0.070	2.91	3.41	2.82	2.70	<u>2.73</u>	2.75	2.73	3.87	3.17	3.42
m4 quarterly	<u>1.18</u> ± 0.013	1.22	1.25	<u>0.965</u>	<u>1.40</u>	1.17	1.17	1.17	1.81	1.24	1.25
m4 yearly	<u>3.46</u> ± 0.076	3.51	3.69	2.55	<u>3.37</u>	3.18	3.04	3.07	4.89	3.69	3.80
m5	0.904 ± 0.001	<u>0.915</u>	0.920	0.919	0.919	0.927	0.927	0.924	1.10	0.934	0.931
nn5	0.563 ± 0.007	<u>0.576</u>	0.583	0.608	0.629	0.665	0.586	0.638	<u>0.998</u>	0.594	0.618
nn5 weekly	0.913 ± 0.010	0.916	0.927	0.865	0.949	<u>0.882</u>	0.979	0.939	0.994	0.941	0.946
tourism monthly	<u>1.47</u> ± 0.014	1.53	1.61	1.62	1.92	1.46	1.65	1.75	3.21	1.84	1.93
tourism quarterly	<u>1.64</u> ± 0.026	1.76	1.84	1.80	2.06	1.59	1.82	1.92	3.77	1.81	1.77
tourism yearly	3.50 ± 0.100	3.69	3.89	3.49	<u>3.23</u>	3.02	3.21	3.15	3.56	3.84	3.98
traffic	0.799 ± 0.013	0.784	0.860	<u>0.726</u>	<u>0.641</u>	<u>0.791</u>	0.758	0.768	0.835	0.812	0.831
weather	0.790 ± 0.008	0.812	<u>0.802</u>	0.822	0.913	0.811	0.810	0.823	<u>0.896</u>	0.809	0.850

Table 18: WQL scores of different zero-shot models on the Chronos-ZS benchmark datasets. The models achieving the **best** and **second-best** scores are highlighted. Results for datasets that are part of the training data for the respective models are shaded in grey, and these results are excluded from the calculation of the best score. We trained TiRex with 6 different seeds and report the observed standard deviation in the plot.

	TiRex	Chronos Bolt B	Chronos Bolt S	TimesFM 2.0	TimesFM 1.0	TabPFN-TS	Moirai L 1.1	Moirai B 1.1	TTM-r2	Chronos B	Chronos S
ETTh	0.079 ± 0.003	0.071	<u>0.076</u>	0.085	0.092	0.098	0.082	0.091	0.118	0.080	0.083
ETThm	0.054 ± 0.001	<u>0.052</u>	0.051	<u>0.052</u>	0.084	0.077	0.070	0.076	0.076	0.070	0.063
australian electricity	0.059 ± 0.005	0.036	<u>0.042</u>	0.067	0.089	0.045	0.038	0.054	0.074	0.067	0.072
car parts	<u>0.990</u> ± 0.010	0.995	1.01	1.65	1.04	0.949	0.990	1.02	1.38	1.07	1.03
cif 2016	<u>0.012</u> ± 0.002	0.016	0.016	0.053	0.020	0.009	0.015	0.016	0.038	<u>0.012</u>	<u>0.012</u>
covid deaths	0.037 ± 0.004	0.047	0.043	0.215	0.204	<u>0.040</u>	0.036	0.045	0.108	0.045	0.063
dominick	0.321 ± 0.001	0.345	0.348	0.371	0.412	0.335	0.344	0.343	0.552	<u>0.331</u>	0.336
ercot	0.019 ± 0.002	0.021	0.026	0.021	0.021	0.020	0.017	0.018	0.044	0.013	<u>0.015</u>
exchange rate	0.013 ± 0.002	0.012	<u>0.011</u>	0.015	0.013	0.010	<u>0.011</u>	<u>0.011</u>	0.377	0.012	<u>0.012</u>
fred md	0.023 ± 0.006	0.042	0.037	0.027	0.036	0.055	0.042	0.050	0.050	<u>0.020</u>	0.015
hospital	<u>0.052</u> ± 0.000	0.057	0.058	0.050	<u>0.052</u>	0.063	0.059	0.058	0.079	0.056	0.057
m1 monthly	0.136 ± 0.004	0.139	0.134	<u>0.130</u>	0.123	0.150	0.177	0.169	0.215	0.131	0.138
m1 quarterly	0.099 ± 0.004	0.101	0.094	0.113	0.087	<u>0.090</u>	0.093	0.076	0.156	0.102	0.106
m1 yearly	<u>0.135</u> ± 0.008	0.151	0.157	0.145	0.163	0.118	0.127	0.123	0.246	0.198	0.183
m3 monthly	0.091 ± 0.000	0.093	0.094	0.089	0.098	<u>0.090</u>	0.099	0.101	0.153	0.096	0.100
m3 quarterly	<u>0.070</u> ± 0.000	0.076	0.077	0.075	0.072	0.067	0.070	0.070	0.115	0.074	0.080
m3 yearly	0.131 ± 0.004	<u>0.129</u>	0.155	0.144	0.123	0.130	0.130	0.131	0.191	0.149	0.157
m4 quarterly	0.074 ± 0.000	0.077	0.078	<u>0.062</u>	<u>0.085</u>	<u>0.075</u>	0.076	0.076	0.125	0.083	0.083
m4 yearly	<u>0.119</u> ± 0.002	0.121	0.128	<u>0.091</u>	<u>0.117</u>	0.114	0.108	0.109	0.192	0.135	0.138
m5	0.551 ± 0.001	0.562	0.567	<u>0.557</u>	0.561	0.565	0.594	0.583	0.668	0.585	0.586
nn5	0.146 ± 0.002	<u>0.150</u>	0.151	0.155	0.160	0.173	0.152	0.165	<u>0.311</u>	0.162	0.169
nn5 weekly	0.083 ± 0.001	0.084	0.085	0.079	0.086	<u>0.081</u>	0.091	0.089	0.113	0.089	0.089
tourism monthly	0.077 ± 0.002	0.090	0.094	0.085	0.101	<u>0.084</u>	0.098	0.099	0.283	0.101	0.108
tourism quarterly	0.061 ± 0.002	<u>0.065</u>	0.067	0.070	0.085	0.093	0.067	0.070	0.200	0.077	0.070
tourism yearly	0.148 ± 0.006	0.166	0.168	<u>0.163</u>	0.148	0.148	0.137	0.138	0.212	0.199	0.201
traffic	0.235 ± 0.004	<u>0.231</u>	0.252	<u>0.212</u>	<u>0.185</u>	0.229	0.236	0.238	5.54	0.255	0.258
weather	0.127 ± 0.000	0.134	0.133	0.133	0.150	<u>0.132</u>	0.133	0.135	0.159	0.137	0.147